

1997

Chemical characteristics of continental outflow from Asia to the troposphere over the western Pacific Ocean during February-March 1994: Results from PEM-West B

R. W. Talbot

J. E. Dibb

B. L. Lefer

J. D. Bradshaw

S. T. Sandholm

See next page for additional authors

Follow this and additional works at: <https://digitalcommons.uri.edu/gsofacpubs>

Citation/Publisher Attribution

Talbot, R. W., et al. (1997), Chemical characteristics of continental outflow from Asia to the troposphere over the western Pacific Ocean during February-March 1994: Results from PEM-West B, *J. Geophys. Res.*, 102(D23), 28255–28274, doi: 10.1029/96JD02340.

Available at: <https://doi.org/10.1029/96JD02340>

This Article is brought to you by the University of Rhode Island. It has been accepted for inclusion in Graduate School of Oceanography Faculty Publications by an authorized administrator of DigitalCommons@URI. For more information, please contact digitalcommons-group@uri.edu. For permission to reuse copyrighted content, contact the author directly.

Chemical characteristics of continental outflow from Asia to the troposphere over the western Pacific Ocean during February-March 1994: Results from PEM-West B

Authors

R. W. Talbot, J. E. Dibb, B. L. Lefer, J. D. Bradshaw, S. T. Sandholm, D. R. Blake, N. J. Blake, G. W. Sachse, J. E. Collins Jr., Brian G. Heikes, John Merrill, G. L. Gregory, B. E. Anderson, H. B. Singh, D. C. Thornton, A. R. Bandy, and R. F. Pueschel

Terms of Use

All rights reserved under copyright.

Chemical characteristics of continental outflow from Asia to the troposphere over the western Pacific Ocean during February - March 1994: Results from PEM-West B

R. W. Talbot,¹ J. E. Dibb,¹ B. L. Lefer,¹ J. D. Bradshaw,² S. T. Sandholm,² D. R. Blake,³ N. J. Blake,³ G. W. Sachse,⁴ J. E. Collins, Jr.,⁴ B. G. Heikes,⁵ J. T. Merrill,⁶ G. L. Gregory,⁴ B. E. Anderson,⁴ H. B. Singh,⁶ D. C. Thornton,⁷ A. R. Bandy,⁷ and R. F. Pueschel⁶

Abstract. We present here the chemical composition of outflow from the Asian continent to the atmosphere over the western Pacific basin during the Pacific Exploratory Mission - West (PEM-West B) in February-March 1994. Comprehensive measurements of important tropospheric trace gases and aerosol particulate matter were performed from the NASA DC-8 airborne laboratory. Backward 5 day isentropic trajectories were used to partition the outflow from two major source regions: continental north ($>20^{\circ}\text{N}$) and continental south ($<20^{\circ}\text{N}$). Air parcels that had not passed over continental areas for the previous 5 days were classified as originating from an aged marine source. The trajectories and the chemistry together indicated that there was extensive rapid outflow of air parcels at altitudes below 5 km, while aged marine air was rarely encountered and only at $<20^{\circ}\text{N}$ latitude. The outflow at low altitudes had enhancements in common industrial solvent vapors such as C_2Cl_4 , CH_3CCl_3 , and C_6H_6 , intermixed with the combustion emission products C_2H_2 , C_2H_6 , CO , and NO . The mixing ratios of all species were up to tenfold greater in outflow from the continental north compared to the continental south source region, with ^{210}Pb concentrations reaching 38 fCi (10^{-15} curies) per standard cubic meter. In the upper troposphere we again observed significant enhancements in combustion-derived species in the 8-10 km altitude range, but water-soluble trace gases and aerosol species were depleted. These observations suggest that ground level emissions were lofted to the upper troposphere by wet convective systems which stripped water-soluble components from these air parcels. There were good correlations between C_2H_2 and CO and C_2H_6 ($r^2 = 0.70 - 0.97$) in these air parcels and much weaker ones between C_2H_2 and H_2O_2 or CH_3OOH ($r^2 \approx 0.50$). These correlations were the strongest in the continental north outflow where combustion inputs appeared to be recent (1 - 2 days old). Ozone and PAN showed general correlation in these same air parcels but not with the combustion products. It thus appears that several source inputs were intermixed in these upper tropospheric air masses, with possible contributions from European or Middle Eastern source regions. In aged marine air mixing ratios of O_3 (≈ 20 parts per billion by volume) and PAN (≤ 10 parts per trillion by volume) were nearly identical at <2 km and 10 - 12 km altitudes due to extensive convective uplifting of marine boundary layer air over the equatorial Pacific even in wintertime. Comparison of the Pacific Exploratory Mission-West A and PEM-West B data sets shows significantly larger mixing ratios of SO_2 and H_2O_2 during PEM-West A. Emissions from eruption of Mount Pinatubo are a likely cause for the former, while suppressed photochemical activity in winter was probably responsible for the latter. This comparison also highlighted the twofold enhancement in C_2H_2 , C_2H_6 , and C_3H_8 in the continental north outflow during PEM-West B. Although this could be due to reduced OH oxidation rates of these species in wintertime, we argue that increased source emissions are primarily responsible.

1. Introduction

The eastward transport of dust-laden air from over the Asian continental and across the marine boundary layer of the North Pacific Ocean is well established [Duce *et al.*, 1980; Prospero *et al.*, 1985; Merrill, 1989; Merrill *et al.*, 1989; Gao *et al.*, 1992]. This aeolian transport occurs north of 20°N and peaks during the spring, a time period characterized by low rainfall and increased frequency of high surface winds associated with the passage of cold fronts over Asia. This transport regime, coupled with the recent accelerating industrialization of the Pacific rim region should produce significant outflow of anthropogenic emissions to the North Pacific troposphere. The sampling of these emissions and an assessment of their impact on atmospheric chemistry over the Pacific was the focus of the NASA Pacific Exploratory Mission - West (PEM-West B).

¹Institute for the Study of Earth, Oceans, and Space, University of New Hampshire, Durham.

²School of Earth and Atmospheric Sciences, Georgia Institute of Technology, Atlanta.

³Department of Chemistry, University of California, Irvine.

⁴NASA Langley Research Center, Hampton, Virginia.

⁵Center for Atmospheric Chemistry, University of Rhode Island, Narragansett.

⁶NASA Ames Research Center, Moffett Field, California.

⁷Department of Chemistry, Drexel University, Philadelphia, Pennsylvania.

Previously, we reported the chemical characteristics of Asian outflow during the fall period, when the outflow of materials is minimized due to an extensive ridge of high pressure over the central western Pacific [Talbot et al., 1996a]. The persistence of this high brings a low-altitude easterly flow of aged marine air to the Pacific rim region, significantly hindering outflow of continental boundary layer air to the North Pacific. The chemical composition of these aged marine air masses was characterized for the PEM-West A September to October study period [Gregory et al., 1996].

During PEM-West A the vertical distributions of CO, C₂H₆, NO_x, and various halocarbon compounds showed regions of outflow at altitudes from 8 to 12 km and below 2 km in nearshore areas. Above 10 km altitude there were substantial enhancements of many species, except water-soluble ones. In general, the chemical characteristics of free tropospheric air was consistent with a transport mechanism of wet vertical convection over the Asian continent coupled with rapid westerly advection by high wind speeds aloft (60 - 70 m s⁻¹).

During springtime the large high-pressure system located over the central North Pacific during other times of the year is displaced eastward. Thus rapid and direct boundary layer outflow of natural and anthropogenic trace gases and aerosol particles is common. In this paper we summarize the chemical characteristics of this extensive material export across the North Pacific. The PEM-West A and B data represent the first comprehensive chemical documentation of the composition of Asian outflow. These data therefore are an important benchmark in the anticipated scheme of heightened anthropogenic activities in the Pacific rim region over the next few decades.

2. Experiment

The airborne component of PEM-West B was conducted aboard the NASA Ames DC-8 research aircraft. Transit and intensive site science missions composed 16 flights, each averaging about 8 hours in duration and covering the altitude range of 0.3 to 12.5 km. The flights over the western Pacific Ocean, from which the data for this paper are drawn, were centered in the geographic grid approximately bounded by 0° - 60°N latitude and 110° - 180°E longitude. A geographic representation of the study region is shown in Figure 1. The base of operation for these missions progressed from (1) Guam (four missions) to (2) Hong Kong (two missions) and on to (3) Yokota, Japan (four missions). Data obtained on transit flights between these locations was also utilized in this paper.

The overall scientific rationale and description of the individual aircraft missions is described in the PEM-West B overview paper [Hoell et al., this issue]. The features of the large-scale meteorological regime and associated air mass trajectory analyses for the February-March 1994 time frame are presented by Merrill et al. [this issue]. Since we present here a broad description of the observed chemistry in continental outflow air masses during PEM-West B, it is impractical to provide species-specific measurement details. Instead, the philosophy was adopted to present a summary of this information in the PEM-West B overview paper [Hoell et al., this issue]. Additional measurement related information for individual species is also summarized in numerous companion papers in this issue. Because of questions regarding the exact suite compounds being measured by current total reactive nitrogen (NO_x) instruments [Sandholm et al., 1996b], we use the sum of the species-specific measurements to

represent NO_x ($\Sigma\text{NO}_x = \text{nitric oxide [NO]} + \text{nitrogen dioxide [NO}_2\text{]} + \text{nitric acid [HNO}_3\text{]} + \text{peroxyacetylnitrate [PAN]} + \text{aerosol nitrate [NO}_3\text{-]}$). Since NO₂ was not measured during PEM-West B, its mixing ratio was calculated using a 1-dimensional time-dependent photochemical model [Crawford et al., this issue].

3. Formulation of Continental Outflow Data Set

3.1 Meteorological Basis

The detailed synoptic meteorological setting leading to outflow of Asian continental air masses over the western Pacific Ocean has been described by Merrill [1989; Merrill et al., 1989]. This section provides a brief description of the large-scale meteorological features during the February-March 1994 time frame.

In the middle to upper troposphere (>500 mbar) there was strong westerly flow off the Asian continent. This direct westerly flow was primarily confined to the 20° - 50°N latitude band, with its focal point centered at 30°N. Rapid westerly flow occurred in this altitude region due to the influence of the Japan (polar) jet [Merrill et al., 1989; Kritz et al., 1990].

Along the Pacific rim at low altitude (<500 mbar) the flow was generally westerly, being constantly diverted around anticyclones approaching from the north or south into the 20° - 50°N latitude band. Direct continental outflow was sampled at low altitude (<7 km) on numerous flights flying over the western Pacific within a few hundred kilometers or less from the Asian continent. Precipitation was associated with many anticyclonic systems as they proceeded across the western Pacific. Often these precipitation-modified air masses were directed to the region north of Guam (≈15° - 25°N and 130° - 140°W) where we sampled it on two flights. Several flights based out of Yokota offered this same opportunity in the 30° - 50°N region.

Air masses were also sampled during PEM-West B over the South China and Celebes Seas. These air masses typically passed over southeastern Asia or the various island chains surrounding this study region. The only opportunities to sample aged Pacific marine air occurred on flights conducted in the geographic region between the Philippine Islands, New Guinea, and Guam. Air masses originating in the equatorial Pacific region are brought to this area by anticyclones traveling in the easterly flow of the nearby intertropical convergence zone (ITCZ).

3.2 Measurement Database

Extensive processing of final archived data was required to obtain the data products utilized in our analysis here. Archived data for each species measured in PEM-West B is maintained by the NASA Global Tropospheric Chemistry project office at Langley Research Center in Hampton, Virginia. Because of extreme diversity in measurement time resolutions for the various species of interest, merged data products were produced for several desired intervals. These data products were generated at the Georgia Institute of Technology (GIT) under the supervision of S. Sandholm and J. Bradshaw. We utilized 30 s averaged data that correspond to the highest-resolution GIT NO measurements in this paper, with the NO data filtered to correspond to a solar zenith angle of 0° - 60°. It should be noted that the chemiluminescence NO measurements reported by Kondo et al. [this issue] were indistinguishable from the GIT two-photon laser-induced fluorescence values utilized here. The measurements of faster response instruments (e.g., meteorological parameters and chemical species, including O₃, CO, CO₂, CH₄, N₂O, condensa-

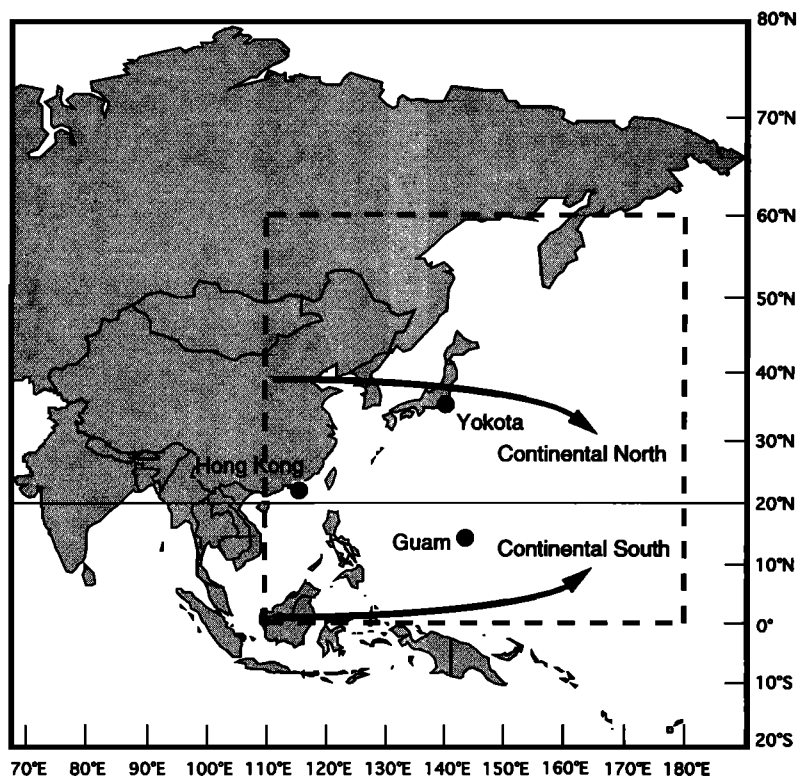


Figure 1. Geographic representation of the PEM-West B study area showing the continental north and continental south source regions. The line at 20°N denotes the geographic division of these two source regions.

tion nuclei (CN), and aerosol number density (aerosols)) were averaged to correspond to the 30-s-based time intervals.

Merged data products on various other time resolutions were utilized for species with longer time resolutions (e.g., sulfur gases, acidic gases, peroxides, PAN, hydrocarbons, and aerosol species). The hydrocarbon data are from measurements reported by *Blake et al.* [this issue].

For all species their limit of detection value was used for measurement periods where the mixing ratio was reported as below the limit of detection. For the two continental outflow air mass classifications presented in this paper (section 3.3) the mixing ratios of most species were generally well above their stated limit of detection. The limit of detection values were primarily utilized in the aged marine air classification database (>5 days since over land).

3.3 Classification of Database

Backward 5 day isentropic trajectories were utilized to identify time intervals that corresponded to constant altitude flight legs where the sampled air parcels had recently passed over continental areas [*Merrill et al.*, this issue]. Spiral data were not utilized in our analysis due to heterogeneity in air masses and practical limitations imposed by the vertical density of trajectories. Overall, the data utilized in this paper represent approximately 65% of the measurement intervals during PEM-West B. An analysis of the PEM-West B data using measurements obtained during selected spirals yielded results similar to those presented here [*Gregory et al.*, this issue]. Thus the presentation of the PEM-West B data here appears to be quite representative of tropospheric chemistry over the western Pacific basin in wintertime.

In our PEM-West A outflow analysis, classifications were defined for <2, 2 - 4, and >5 days since the air masses had passed

over landmasses based on back trajectory information. Vertical grouping were for three altitude regions of <2, 2 - 7, and 7 - 12.5 km. We further divided the vertical air mass classifications into two groups referred to as "continental north" and "continental south." The dashed line in Figure 1 indicates the 20°N division between the two source regions. It is likely that the latitudinal differences in these air masses' histories exposed them to various amounts and types of continental emissions which should be reflected in their chemical compositions. To allow direct comparison to the PEM-West A data, this same air mass classification scheme was used for PEM-West B (Figure 2).

Examination of the back trajectories for the PEM-West B study period indicated that the outflow was in most cases quite rapid (<2 days). This is distinctly different from what was observed in PEM-West A. Upon breaking the data into the various classifications defined above, the 2 - 4 day cases did not contain a sufficient amount of data (i.e., < 2 hours of data) for meaningful interpretive purposes. Thus we compare here three main air mass classifications: continental north (<2 days), continental south (< 2 days), and aged marine (>5 days).

4. Chemical Characteristics of Air Mass Classifications

Throughout this section we use the term "enhanced" to indicate when a species mixing ratio was greater than two standard deviations above their mean background one. We determined the background mixing ratio using the data that represent the smallest one third of the measurements at a given altitude. In most cases this produced a species vertical distribution that was synonymous with that in the aged marine air classification (i.e., air that has not passed over continental areas for at least 5 days).

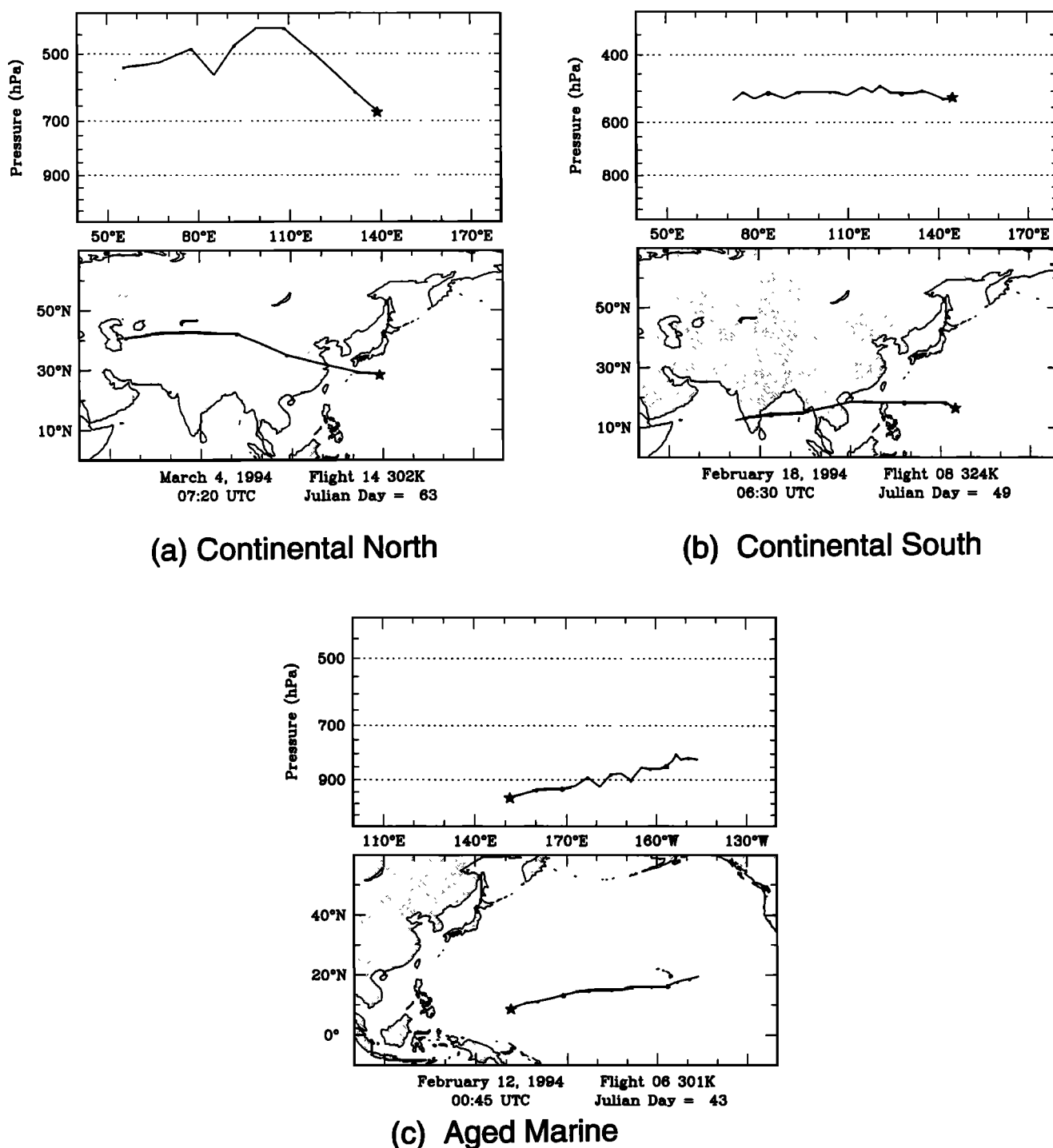


Figure 2. Examples of isentropic backward trajectories used to partition air masses into (a) continental north, (b) continental south, or (c) aged marine classifications.

4.1. Continental North Source Region

The largest mixing ratios of most chemical species over the western Pacific were observed at altitudes below 5 km (Table 1), with enriched layers centered at 0.5 and 3 km (Figure 3). These low-altitude plumes were the most pronounced for aerosols (Figure 3a) and the water-soluble species (Figure 3b). On several flights the plumes at 0.5 km altitude contained very large numbers ($\approx 10^4 \text{ cm}^{-3}$) of CN, indicative of recent combustion emissions.

These plumes also exhibited the largest ratio values for $\text{C}_3\text{H}_8/\text{C}_2\text{H}_6$ and $\text{C}_2\text{H}_2/\text{CO}$, again suggesting recent combustion emissions [McKeen and Liu, 1993; Smyth *et al.*, 1996]. The coincident enhancements in the mixing ratios of C_2Cl_4 , CH_3CCl_3 , and C_2H_6 (Figure 3c) suggest that anthropogenic sources contributed significantly to the composition of the outflowing air parcels [Wang *et al.*, 1995].

Ozone mixing ratios at altitudes < 5 km were generally 40 - 45 parts per billion by volume (ppbv) (Table 1). In only one case did

Table 1. Mixing Ratios of Principal Species Measured in Fresh (< 2 days) Asian Continental-North Outflow for Isentropic Back Trajectories Originating > 20°N Latitude

| Species | < 2 km | | | | 2 - 7 km | | | | 7 - 12 km | | | | | | |
|---|--------|------|--------|-------------|----------|-------|------|--------|-------------|------|-------|------|--------|-------------|------|
| | Mean | s.d. | Median | Range | N | Mean | s.d. | Median | Range | N | Mean | s.d. | Median | Range | N |
| NO | 31 | 67 | 18 | 3.1-937 | 690 | 16 | 18 | 13 | 2.6-568 | 1466 | 49 | 68 | 39 | 7.4-833 | 987 |
| HNO ₃ | 617 | 1263 | 229 | 30-6596 | 74 | 168 | 166 | 126 | 37-1115 | 152 | 166 | 69 | 146 | 62-389 | 75 |
| PAN | 559 | 434 | 134 | 54-2187 | 65 | 289 | 190 | 108 | 1.7-885 | 186 | 177 | 164 | 98 | 20-965 | 152 |
| ΣNO _x | 1084 | 1587 | 624 | 123-10243 | 74 | 449 | 305 | 406 | 64-1923 | 152 | 473 | 208 | 449 | 153-1033 | 75 |
| O ₃ | 44 | 9 | 42 | 34-144 | 860 | 46 | 6 | 45 | 23-69 | 2285 | 55 | 15 | 51 | 25-119 | 1818 |
| CO | 206 | 68 | 186 | 145-623 | 800 | 145 | 45 | 138 | 72-300 | 2065 | 112 | 45 | 94 | 62-316 | 1529 |
| CH ₄ | 1810 | 24 | 1805 | 1771-2051 | 795 | 1771 | 35 | 1760 | 1707-1884 | 1736 | 1736 | 20 | 1723 | 1706-1808 | 1356 |
| CO ₂ | 364.0 | 2.5 | 363.7 | 360.8-390.0 | 810 | 360.7 | 1.8 | 360.5 | 357.6-366.0 | 2106 | 358.7 | 1.2 | 358.2 | 356.7-363.4 | 1632 |
| N ₂ O | 312.0 | 0.39 | 311.9 | 310.9-312.7 | 291 | 311.6 | 0.75 | 311.6 | 309.8-314.1 | 891 | 311.2 | 0.90 | 311.4 | 308.2-313.0 | 652 |
| SO ₂ | 1222 | 4686 | 104 | 26-29770 | 93 | 153 | 245 | 22 | 5-1432 | 234 | 25 | 8.5 | 22 | 5-62 | 173 |
| CH ₃ SCH ₃ | 9.4 | 6.4 | 5.2 | 1.1-25 | 92 | 1.3 | 2.4 | 2.3 | 2.1-14.7 | 227 | ND | ND | ND | ND | 173 |
| HCOOH | 514 | 787 | 254 | 11-4001 | 98 | 224 | 458 | 113 | 11-2953 | 177 | 131 | 90 | 102 | 11-508 | 100 |
| CH ₃ COOH | 589 | 947 | 264 | 16-4587 | 98 | 239 | 493 | 113 | 16-4321 | 177 | 131 | 102 | 95 | 16-620 | 102 |
| H ₂ O ₂ | 737 | 752 | 460 | 99-3494 | 120 | 671 | 852 | 335 | 53-5790 | 302 | 298 | 350 | 155 | 30-1812 | 205 |
| CH ₃ OOH | 157 | 130 | 122 | 23-579 | 120 | 223 | 202 | 144 | 28-1205 | 303 | 131 | 116 | 53 | 19-528 | 156 |
| Ethane | 2337 | 377 | 2294 | 1582-4323 | 137 | 1592 | 674 | 1614 | 469-3771 | 324 | 874 | 426 | 672 | 439-2463 | 252 |
| Ethene | 183 | 316 | 94 | 26-3597 | 138 | 52 | 57 | 33 | 3.0-536 | 313 | 30 | 52 | 6.7 | 3.1-238 | 212 |
| Propane | 961 | 314 | 888 | 355-2460 | 138 | 479 | 358 | 422 | 38-1678 | 324 | 131 | 115 | 64 | 35-558 | 252 |
| i-Butane | 173 | 78 | 151 | 42-684 | 137 | 83 | 69 | 53 | 3.0-338 | 285 | 19 | 15 | 4.4 | 3.1-75 | 142 |
| n-Butane | 330 | 156 | 291 | 72-1342 | 137 | 149 | 131 | 101 | 3.0-618 | 303 | 25 | 27 | 6.8 | 3.0-128 | 190 |
| Ethyne | 908 | 356 | 792 | 463-3356 | 137 | 477 | 278 | 471 | 28-1481 | 324 | 235 | 270 | 131 | 35-1513 | 252 |
| i-Pentane | 89 | 93 | 70 | 25-1086 | 137 | 39 | 34 | 17 | 3.6-189 | 249 | 8.6 | 6.1 | 3.5 | 3.1-27 | 79 |
| n-Pentane | 58 | 47 | 46 | 12-474 | 137 | 26 | 22 | 11 | 3.0-120 | 242 | 7.3 | 3.7 | 5.2 | 3.0-17 | 56 |
| n-Hexane | 16 | 12 | 13 | 3.4-123 | 136 | 9.8 | 5.9 | 4.0 | 3.0-33 | 137 | 4.0 | 0.84 | 2.8 | 3.2-5.2 | 6 |
| Benzene | 180 | 89 | 150 | 89-916 | 137 | 81 | 56 | 74 | 3.8-301 | 321 | 33 | 48 | 13 | 3.1-267 | 238 |
| ¹⁹ F | 276 | 2.0 | 276 | 272-290 | 137 | 274 | 2.4 | 274 | 264-294 | 324 | 272 | 3.3 | 272 | 262-288 | 250 |
| ¹⁸ F | 523 | 3.7 | 523 | 515-554 | 137 | 522 | 4.7 | 522 | 511-554 | 324 | 519 | 3.8 | 520 | 508-539 | 250 |
| ¹³ F | 86 | 1.3 | 86 | 84-94 | 136 | 85 | 1.3 | 85 | 81-91 | 317 | 84 | 2.4 | 84 | 74-87 | 239 |
| CH ₃ CCl ₃ | 134 | 8.0 | 132 | 145-220 | 137 | 125 | 5.5 | 126 | 111-148 | 305 | 119 | 5.0 | 118 | 104-129 | 221 |
| CCl ₄ | 108 | 2.9 | 108 | 105-139 | 136 | 108 | 1.9 | 108 | 100-121 | 309 | 107 | 2.6 | 106 | 97-115 | 220 |
| C ₂ Cl ₄ | 21 | 5.1 | 20 | 9.0-50 | 137 | 13 | 6.1 | 13 | 3.4-27 | 310 | 6.0 | 2.7 | 5.0 | 1.0-14 | 242 |
| C ₂ H ₂ C ₂ H ₆ | 0.40 | 0.07 | 0.39 | 0.18-0.59 | 137 | 0.26 | 0.12 | 0.26 | 0.06-0.47 | 324 | 0.13 | 0.05 | 0.11 | 0.06-0.25 | 252 |
| C ₂ H ₂ CO | 4.4 | 0.67 | 4.2 | 3.2-7.4 | 115 | 3.0 | 1.3 | 2.9 | 0.18-8.6 | 273 | 1.6 | 0.95 | 1.1 | 0.62-5.0 | 215 |
| NO _x | 110 | 85 | 99 | 20-374 | 15 | 56 | 48 | 32 | 6.1-182 | 27 | 36 | 37 | 9.4 | 6.3-121 | 15 |
| nss-SO ₄ ²⁻ | 400 | 220 | 367 | 135-855 | 15 | 179 | 137 | 173 | 11-504 | 32 | 42 | 38 | 20 | 6.2-127 | 25 |
| NH ₄ ⁺ | 579 | 457 | 555 | 47-1837 | 15 | 255 | 218 | 169 | 21-750 | 30 | 106 | 81 | 20 | 20-247 | 13 |
| ²¹⁰ Pb | 17 | 11 | 13 | 5.1-38 | 15 | 11 | 6.3 | 9.7 | 0.60-25 | 32 | 6.8 | 4.0 | 5.3 | 2.9-20 | 25 |
| ⁷ Be | 152 | 76 | 79 | 50-239 | 11 | 227 | 174 | 147 | 27-759 | 26 | 626 | 462 | 489 | 20-1481 | 24 |
| CN | 1850 | 2737 | 1039 | 102-26000 | 777 | 518 | 310 | 401 | 47-3029 | 1937 | 341 | 146 | 227 | 20-1090 | 1206 |
| Aerosols | 55 | 168 | 13 | 3.3-1797 | 882 | 17 | 85 | 1.5 | 0.05-1536 | 2302 | 1.7 | 5.1 | 0.38 | 0.005-71 | 1838 |

Mixing ratios are stated in parts per trillion by volume; except for CO, CH₄, N₂O and O₃ which are in parts per billion by volume; CO₂ in parts per million by volume, and radioisotopes in fempto curies per standard cubic meter. Ratio of C₂H₂/CO is stated in parts per trillion by volume/parts per billion by volume. nssSO₄²⁻, non-sea-salt sulfate. CN, condensation nuclei. Aerosols refers to 0.35 - 2.5 μm diameter particles. NA, not available. ND, not detected.

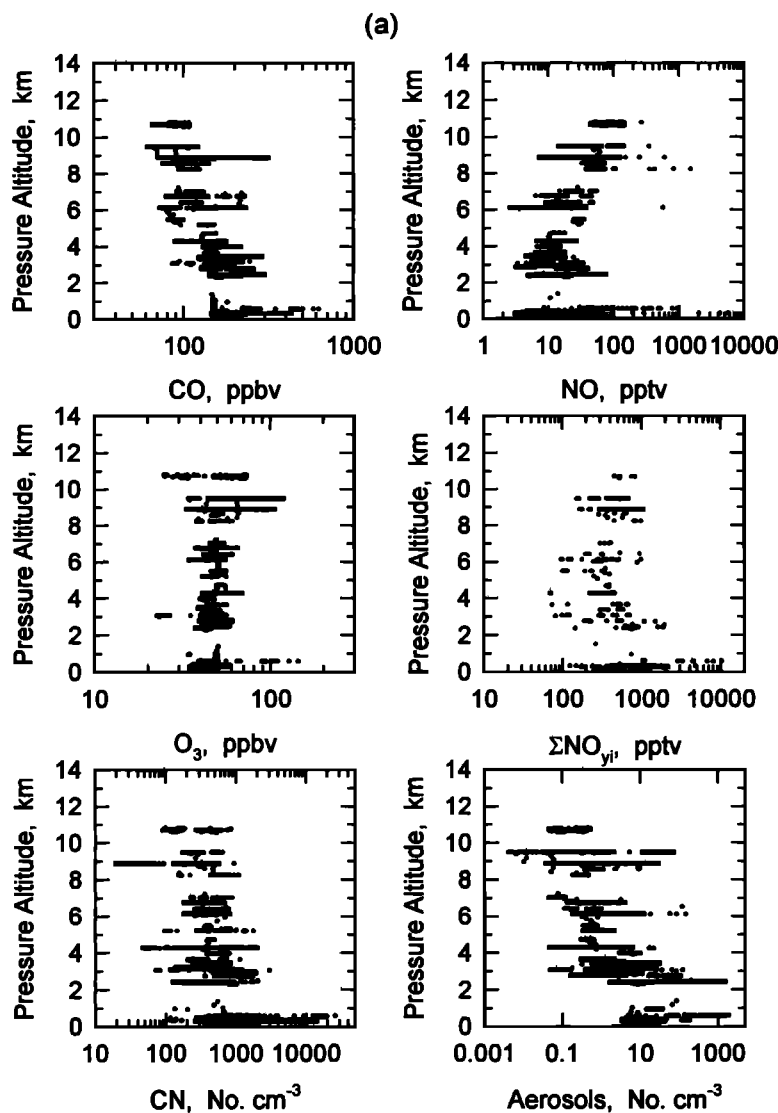


Figure 3. Vertical distributions of selected atmospheric species in outflow air masses originating over the continental north source region. Trajectory analysis [Merrill *et al.*, this issue] indicated that these air masses had spent ≤ 2 days over the western Pacific basin since leaving the Asian continent. Species grouping reflect (a) principal species resulting from combustion processes, (b) water-soluble species, and (c) air mass tracer species.

we encounter O_3 mixing ratios significantly enhanced above this range, and this occurred near Taiwan in heavily polluted air (Figure 3a). These same air parcels contained highly elevated mixing ratios of other photochemically produced species, including PAN, HNO_3 , H_2O_2 , CH_3OOH , $HCOOH$, and CH_3COOH .

The vertical distribution of numerous species showed elevated mixing ratios at altitudes up to 10 km. This effect was particularly noticeable for CO, H_2O_2 , CH_3OOH , PAN, C_2H_2 , C_2H_6 , and C_2Cl_4 . The outflow near 9 km altitude appears to show recent photochemical processing as evidenced by enhancements of O_3 , PAN, H_2O_2 , and CH_3OOH . An anthropogenic combustion influence at this altitude is also apparent given the enhancements in CO, C_2H_2 , and C_2Cl_4 . Although there was not a significant correlation between O_3 and ^{210}Pb in these air parcels, 7Be concentrations and its weak correlation with O_3 ($r^2 = 0.49$) are not indicative of a dominant stratospheric influence either [Dibb *et al.*, this issue].

Aerosols and most of the water-soluble species were not enhanced in these high-altitude air parcels, suggesting that we sampled outflow from wet convection where these species were removed by scavenging processes. Since H_2O_2 and CH_3OOH appear to be enhanced in this outflow, it is likely that at least some photochemical processing (1 - 2 days) occurred at high altitude. Otherwise, one would expect that H_2O_2 and to a lesser extent CH_3OOH would have been scavenged effectively during wet convective transport. Ratio values of CH_3OOH/H_2O_2 are usually >1 in air masses recently influenced (within 1 - 2 days) by wet convective scavenging processes [Heikes, 1992; Talbot *et al.*, 1996b].

An alternative explanation for the observed species enhancements at high altitude could be transport of European emission products to the western Pacific region. Winds speeds of up to 100 m s^{-1} were encountered in the middle to upper troposphere during flights downwind of the continental north source region. Thus

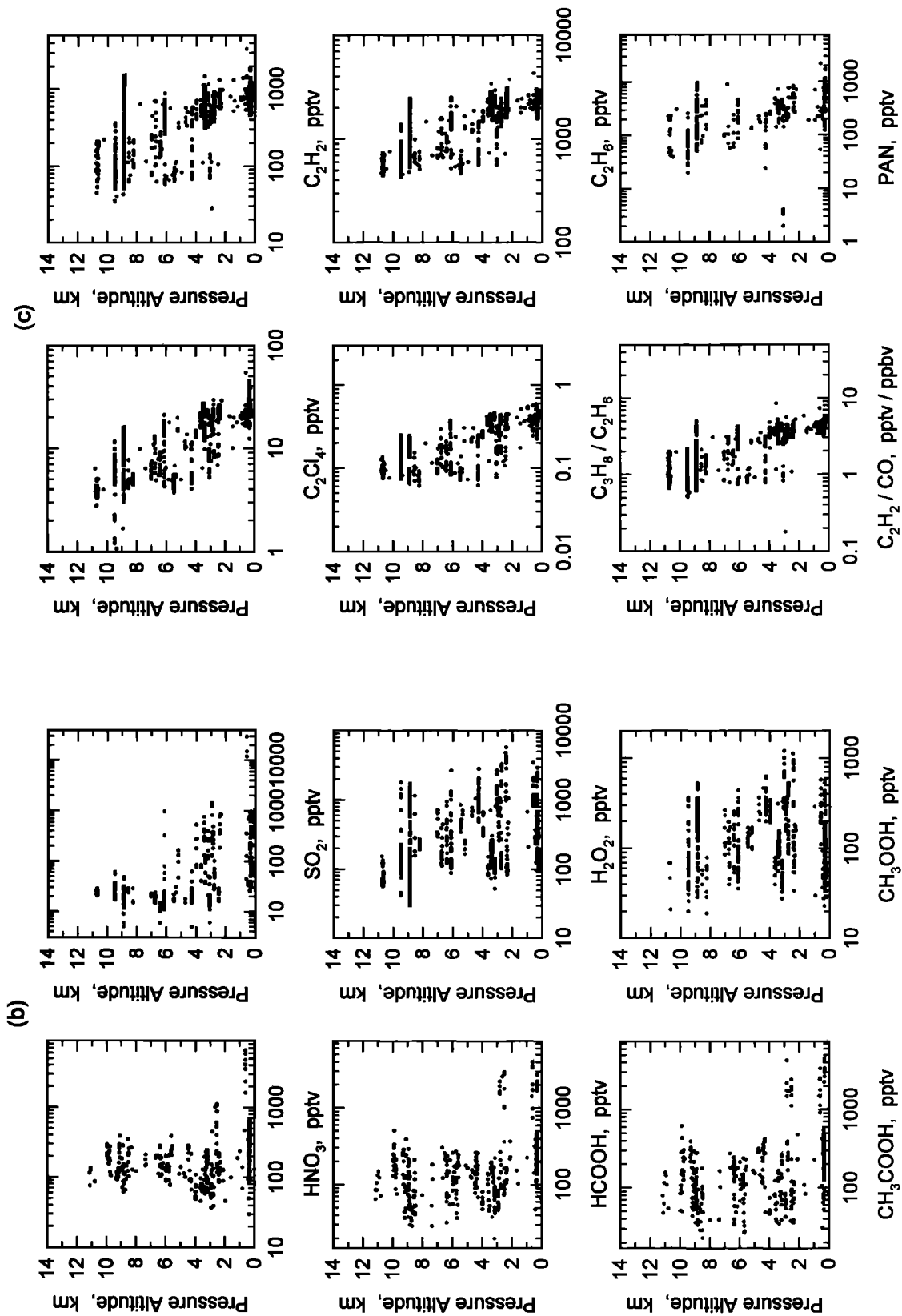


Figure 3. (continued)

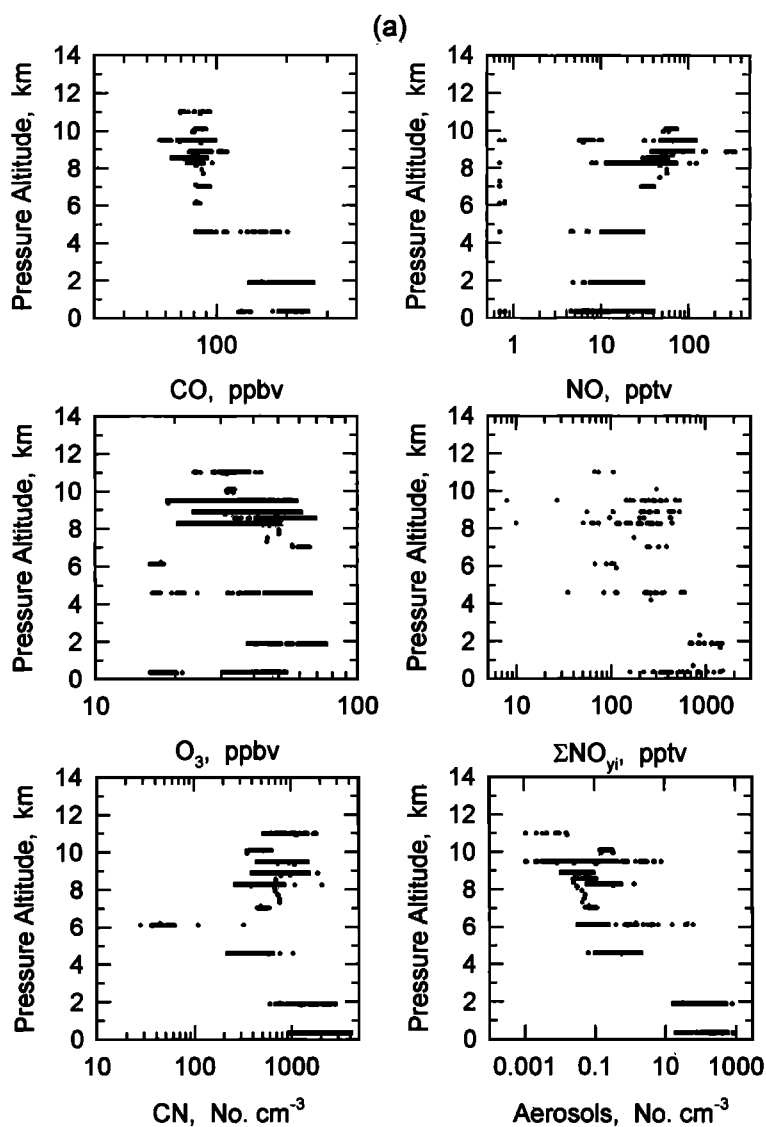


Figure 4. Vertical distributions of selected atmospheric species in outflow air masses originating over the continental south source region. Trajectory analysis [Merrill *et al.*, this issue] indicated that these air masses had spent ≤ 2 days over the western Pacific basin since leaving the Asian continent. Species grouping reflect (a) principal species resulting from combustion processes, (b) water-soluble species, and (c) air mass tracer species.

long-range transport of anthropogenic emissions from European and Middle Eastern source areas could reach the western Pacific in 2 - 3 days, and their importance cannot be ruled out.

4.2. Continental South Source Region

There were both differences and similarities in the vertical distribution of species in air parcels advected over the continental south versus north source regions (Figures 3 and 4). In general, the peak mixing ratios of all species were up to tenfold smaller in the continental south outflow (Table 2). As we found for the continental north outflow, the water-soluble species in the continental south outflow showed enhanced mixing ratios below 6 km and low constant ones above this altitude (Figure 4b).

A striking feature of the continental south data was the relatively constant and low mixing ratios of CO (≈ 85 ppbv), C_2H_6 (≈ 550 pptv), and C_2H_2 (≈ 65 pptv) in the middle to upper troposphere (Figures 4a and 4c). The ratios C_3H_8/C_2H_6 and C_2H_2/CO also had relatively low values in these air masses. The composition of these air parcels were similar to what was observed in aged

marine air at low latitudes over the western Pacific (Figures 6a, 6b, and 6c).

An important aspect of the convective activity over the equatorial western Pacific is that in the upper troposphere it appears to facilitate nucleation of CN aerosols and production of NO from lightning (Figure 4a). Although the enhancements in these materials could be from aircraft emissions [Ehhalt *et al.*, 1992], our flight patterns in the continental south outflow region were not near commercial air traffic routes [Hoell *et al.*, this issue]. Instead, several flights over the western Pacific intercepted convective systems in the equatorial region with coincident large enhancements in NO. Certainly, the meager enhancements in C_2H_2 , C_3H_8/C_2H_6 , or C_2H_2/CO at 9 km altitude do not support the idea of very recent ground level combustion inputs to these air parcels (Figure 4c).

4.3. Species Relationships in Outflow at 8 - 10 km Altitude

The data for the continental north 8.5 - 10 km altitude bin was examined for relationships between selected species to investigate

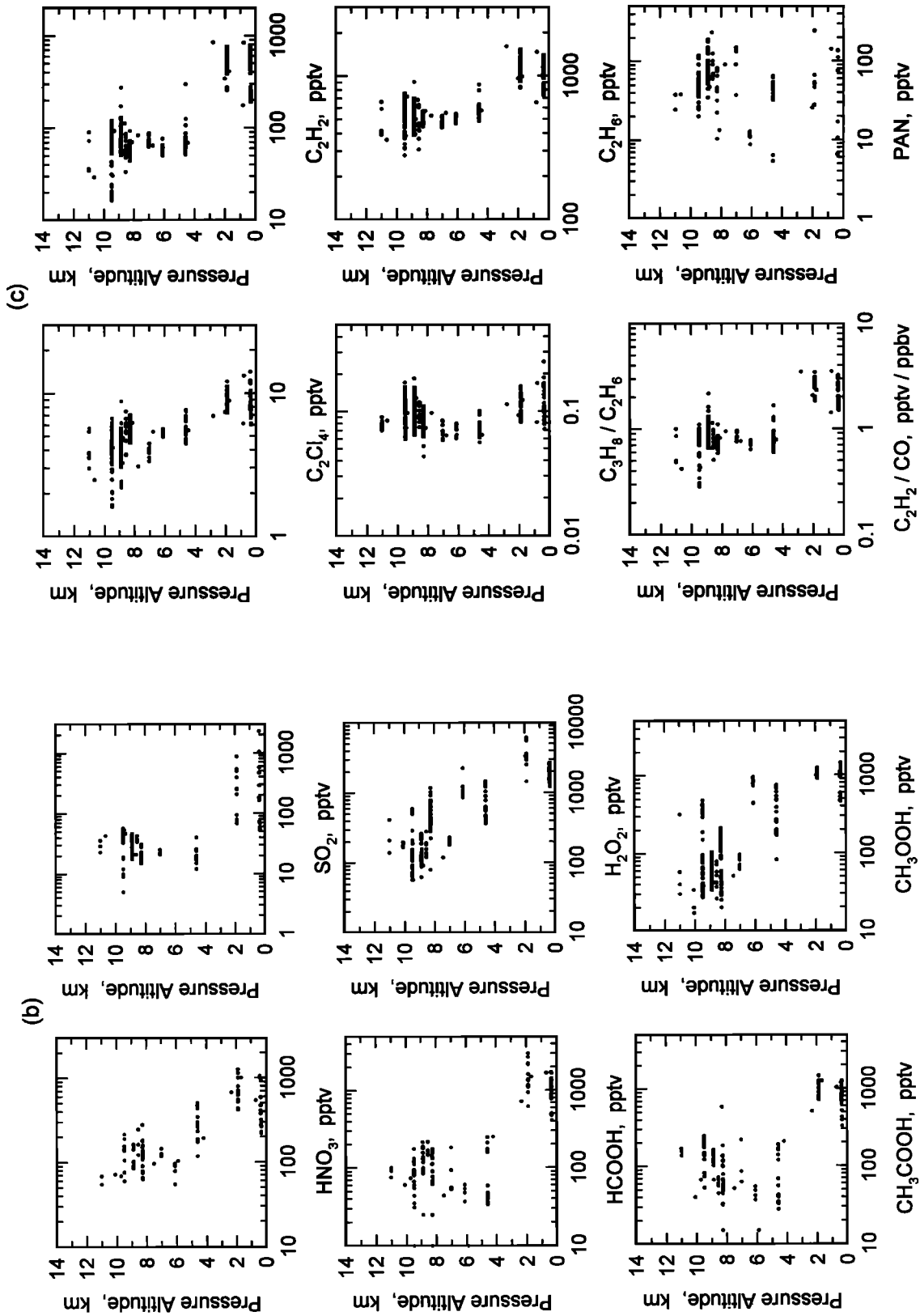


Figure 4. (continued)

Table 2. Mixing Ratios of Principal Species Measured in Fresh (< 2 days) Asian Continental-South Outflow for Isentropic Back Trajectories Originating < 20°N Latitude

| Species | < 2 km | | | | 2 - 7 km | | | | 7 - 12 km | | | | | | | |
|--|--------|------|--------|-------------|----------|-------|------|--------|-------------|-----|-------|------|--------|-------------|--------|---|
| | Mean | s.d. | Median | Range | N | Mean | s.d. | Median | Range | N | Mean | s.d. | Median | Range | N | |
| NO | 13 | 7.8 | 6.8 | 4.6-40 | 238 | 15 | 7.8 | 17 | 4.5-30 | 183 | 57 | 34 | 56 | 7.9-339 | 591 | |
| HNO ₃ | 615 | 316 | 548 | 219-1275 | 32 | 455 | 344 | 421 | 55-1225 | 33 | 124 | 47 | 122 | 55-279 | 55 | |
| PAN | 78 | 82 | 6.4 | 6.4-247 | 20 | 35 | 22 | 13 | 5.4-68 | 29 | 57 | 28 | 38 | 8.8-149 | 98 | |
| ΣNO _y | 941 | 1114 | 721 | 159-7029 | 32 | 279 | 206 | 257 | 75-868 | 33 | 234 | 132 | 243 | 68-540 | 55 | |
| O ₃ | 39 | 15 | 41 | 16-76 | 361 | 46 | 18 | 56 | 16-66 | 300 | 38 | 9 | 35 | 21-69 | 1233 | |
| CO | 182 | 37 | 187 | 125-260 | 310 | 92 | 18 | 88 | 81-203 | 275 | 82 | 7 | 81 | 57-111 | 1029 | |
| CH ₄ | 1756 | 12 | 1755 | 1737-1786 | 179 | 1719 | 11 | 1712 | 1699-758 | 188 | 1714 | 9 | 1712 | 1678-1737 | 997 | |
| CO ₂ | 359.9 | 1.5 | 357.4 | 357.1-363.8 | 196 | 358.1 | 0.24 | 358.0 | 357.7-359.1 | 221 | 357.8 | 0.37 | 357.7 | 357.0-359.0 | 1062 | |
| N ₂ O | NA | NA | NA | NA | NA | NA | NA | NA | NA | NA | 312.1 | 0.28 | 311.9 | 311.6-312.7 | 77 | |
| SO ₂ | 426 | 609 | 68 | 52-2290 | 27 | 17 | 4.3 | 12 | 12-26 | 23 | 29 | 12 | 23 | 5-57 | 130 | |
| CH ₃ SCH ₃ | 13 | 8.9 | 1.2 | 1.1-30 | 22 | 0.85 | 0.62 | 1.1 | 0.90-2.6 | 30 | 0.68 | 0.61 | 0.80 | 0.60-4.7 | 125 | |
| HCOOH | 1276 | 576 | 1153 | 411-3018 | 37 | 127 | 161 | 48 | 10-721 | 20 | 99 | 52 | 91 | 10-218 | 66 | |
| CH ₃ COOH | 904 | 272 | 866 | 328-1487 | 37 | 102 | 114 | 43 | 15-514 | 20 | 120 | 83 | 117 | 15-589 | 69 | |
| H ₂ O ₂ | 2548 | 1183 | 2033 | 1236-6131 | 38 | 782 | 428 | 615 | 364-2251 | 38 | 268 | 225 | 180 | 57-1178 | 149 | |
| CH ₃ OOH | 1008 | 205 | 1022 | 463-1433 | 39 | 425 | 280 | 305 | 82-951 | 38 | 88 | 92 | 54 | 17-481 | 141 | |
| Ethane | 1063 | 219 | 1053 | 655-1528 | 56 | 603 | 186 | 555 | 468-1601 | 41 | 538 | 102 | 543 | 280-912 | 183 | |
| Ethane | 42 | 29 | 35 | 7.4-129 | 56 | 8.6 | 8.1 | 6.4 | 3.4-52 | 40 | 5.7 | 5.8 | 4.6 | 3.0-74 | 157 | |
| Propane | 125 | 56 | 119 | 53-316 | 56 | 45 | 25 | 39 | 29-183 | 41 | 52 | 21 | 47 | 20-126 | 183 | |
| <i>i</i> -Butane | 15 | 13 | 8.6 | 3.3-59 | 54 | 7.0 | 3.9 | 4.5 | 3.8-14 | 6 | 7.0 | 2.8 | 4.3 | 3.0-13 | 62 | |
| <i>n</i> -Butane | 28 | 28 | 15 | 3.1-122 | 56 | 7.9 | 6.9 | 6.7 | 3.1-25 | 11 | 7.4 | 4.2 | 5.1 | 3.0-20 | 103 | |
| Ethyne | 458 | 177 | 464 | 176-835 | 56 | 99 | 133 | 65 | 50-847 | 41 | 70 | 27 | 67 | 16-274 | 183 | |
| <i>i</i> -Pentane | 12 | 9.3 | 4.3 | 3.0-37 | 36 | 5.7 | 1.9 | NA | 4.3-7.0 | 2 | 6.0 | 6.4 | 4.3 | 3.0-26 | 12 | |
| <i>n</i> -Pentane | 8.7 | 5.4 | 5.8 | 3.1-23 | 27 | ND | ND | ND | ND | ND | 4.7 | 2.2 | 5.2 | 3.0-12 | 16 | |
| <i>n</i> -Hexane | ND | ND | ND | ND | ND | ND | ND | ND | ND | ND | ND | ND | ND | ND | ND | |
| Benzene | 78 | 30 | 80 | 27-153 | 56 | 15 | 22 | 10 | 3.2-41 | 40 | 10 | 5.2 | 9.1 | 3.1-40 | 174 | |
| ¹¹ F | 276 | 3.9 | 275 | 271-290 | 56 | 273 | 1.4 | 273 | 270-275 | 41 | 272 | 2.0 | 272 | 266-277 | 182 | |
| ¹² F | 519 | 3.9 | 519 | 513-531 | 56 | 518 | 2.1 | 518 | 513-521 | 41 | 518 | 3.9 | 519 | 505-527 | 181 | |
| ¹⁹ F | 85 | 0.95 | 84 | 84-87 | 56 | 84 | 0.81 | 84 | 84-87 | 41 | 84 | 2.0 | 84 | 75-88 | 178 | |
| CH ₃ CCl ₃ | 140 | 3.2 | 139 | 132-146 | 56 | 132 | 6.1 | 132 | 127-148 | 41 | 132 | 6.1 | 132 | 111-146 | 160 | |
| CCl ₄ | 108 | 1.2 | 108 | 105-110 | 56 | 108 | 1.5 | 107 | 106-113 | 41 | 106 | 2.6 | 106 | 97-111 | 158 | |
| C ₂ Cl ₄ | 7.9 | 1.6 | 7.6 | 5.4-13 | 56 | 5.1 | 0.88 | 5.0 | 4.0-8.0 | 42 | 4.1 | 1.1 | 4.1 | 1.4-7.9 | 169 | |
| C ₃ H ₈ /C ₂ H ₆ | 0.11 | 0.03 | 0.10 | 0.07-0.25 | 56 | 0.07 | 0.01 | 0.07 | 0.06-0.11 | 41 | 0.10 | 0.03 | 0.09 | 0.04-0.18 | 183 | |
| C ₂ H ₂ /CO | 2.4 | 0.55 | 2.4 | 1.4-3.5 | 49 | 0.93 | 0.54 | 0.74 | 0.60-3.5 | 35 | 0.81 | 0.23 | 0.78 | 0.28-2.2 | 149 | |
| NO ₃ ⁻ | 167 | 64 | 148 | 96-254 | 5 | 8.1 | NA | 8.1 | NA | 4 | 1 | 8.3 | 2.6 | 6.7 | 6.4-12 | 4 |
| nss-SO ₄ ²⁻ | 625 | 255 | 620 | 260-950 | 5 | 12 | 1.7 | 12 | 9.1-13 | 4 | 8.2 | 4.9 | 6.9 | 5.4-20 | 16 | |
| NH ₄ ⁺ | 833 | 375 | 913 | 284-1181 | 5 | 18 | 13 | 20 | 15-26 | 3 | 21 | 1.4 | 21 | 20-23 | 4 | |
| ²¹⁰ Pb | 16 | 5.9 | 17 | 8.3-24 | 5 | 4.4 | 2.7 | 4.6 | 0.81-7.8 | 5 | 3.3 | 1.4 | 3.5 | 0.84-6.2 | 17 | |
| ⁷ Be | 204 | 127 | 212 | 129-379 | 5 | 280 | 232 | 265 | 147-442 | 3 | 168 | 112 | 151 | 19-425 | 16 | |
| CN | 1671 | 674 | 1340 | 607-4070 | 313 | 293 | 132 | 303 | 28-1044 | 266 | 670 | 298 | 527 | 270-2304 | 1023 | |
| Aerosols | 142 | 119 | 135 | 18-883 | 361 | 1.1 | 5.0 | 0.45 | 0.03-63 | 303 | 0.15 | 0.53 | 0.06 | 0-14 | 1265 | |

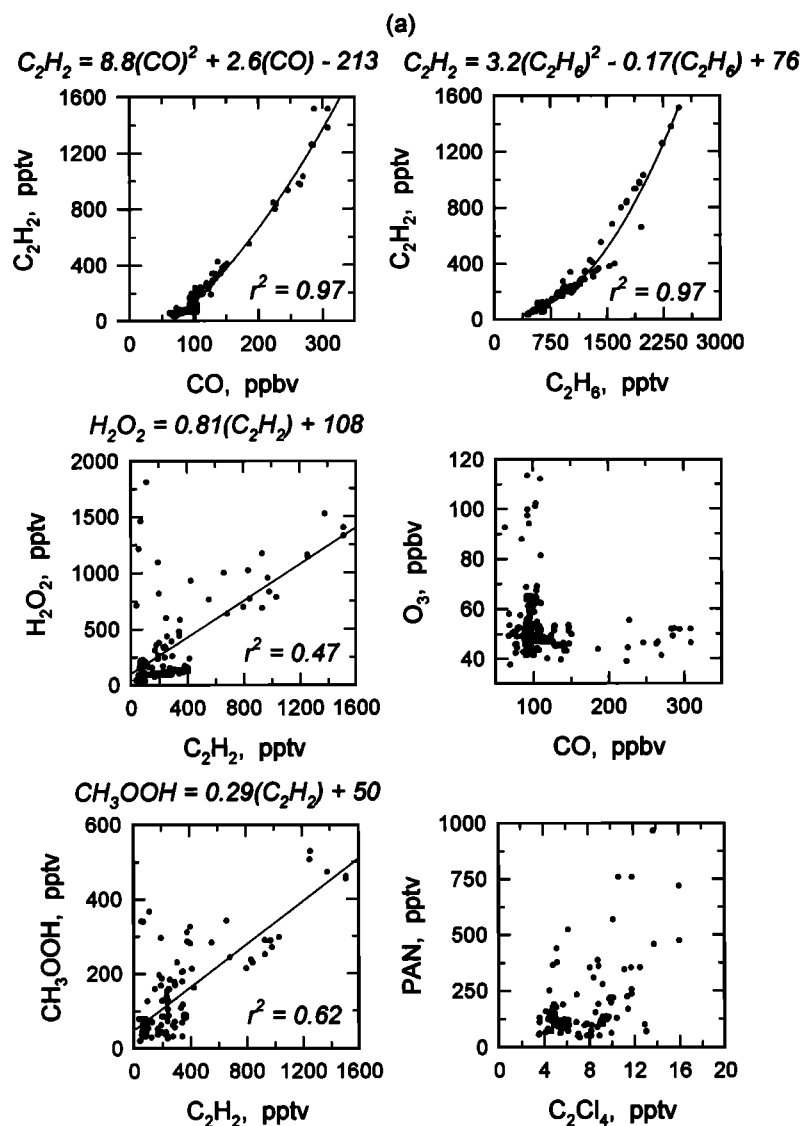


Figure 5. Relationship between selected species in the 8 - 10 km altitude range in the (a) continental north and (b) continental south air mass classifications. The various relationships were fitted with either a linear or a parabolic function depending on which yielded the higher correlation coefficient.

the chemical nature of these upper tropospheric air parcels. The salient relationships found in these air parcels are depicted in Figure 5a. The bulk of these data are from two plumes, with the one at 9 km being the most prominent (Figure 3). The remarkably good correlation between CO and C_2H_2 ($r^2 = 0.97$) indicates a strong combustion influence on the chemical composition of these air parcels. There is also a good correlation between C_2H_2 and C_2H_6 ($r^2 = 0.97$) and weaker ones with H_2O_2 and CH_3OOH ($r^2 = 0.47$ and 0.62 , respectively). Together these relationships are indicative of emissions from fossil fuel or biomass burning, including space heating. Since CH_3Cl , a good tracer for biomass burning [Blake *et al.*, 1996], was not significantly enhanced in these same air parcels, this tends to minimize the chance that this source had a strong influence on the composition of air parcels in the upper troposphere. Furthermore, because of the poor correlation of C_2Cl_4 with C_2H_2 and CO ($r^2 < 0.1$; not shown), it is unlikely that industrial sources had a major impact on the composition of these air parcels.

It is noteworthy that there was no correlation between the combustion product species and O_3 or PAN. This result suggests

that the combustion influence was recent (i.e., within a day or so), with some photochemical processing occurring in this time span. The largest O_3 and PAN mixing ratios were coincident with small ones for CO and C_2H_2 , indicating the intermixing of aged photochemically processed air parcels with the ones recently influenced by combustion emissions. Mixing ratios of $O_3 > 80$ ppbv coincided with concentrations of ${}^7Be \geq 1000$ fCi (10^{-15} Ci) per standard cubic meter (fCi scm^{-1}), indicating a probably stratospheric source for this enhanced O_3 . The enhancements in certain species at 8.5 - 10 km altitude were probably driven by convective uplifting of recent combustion emissions that were subsequently mixed with photochemically aged industrial emissions. These aged industrial emissions may have been advected to the western Pacific by long-range transport from European or Middle Eastern source regions.

The data for the continental south 8 - 10 km altitude bin was also examined for relationships between selected species to investigate the chemical nature of these upper tropospheric air parcels. We present selected species relationships in Figure 5b. Again we found that there was a relatively good correlation

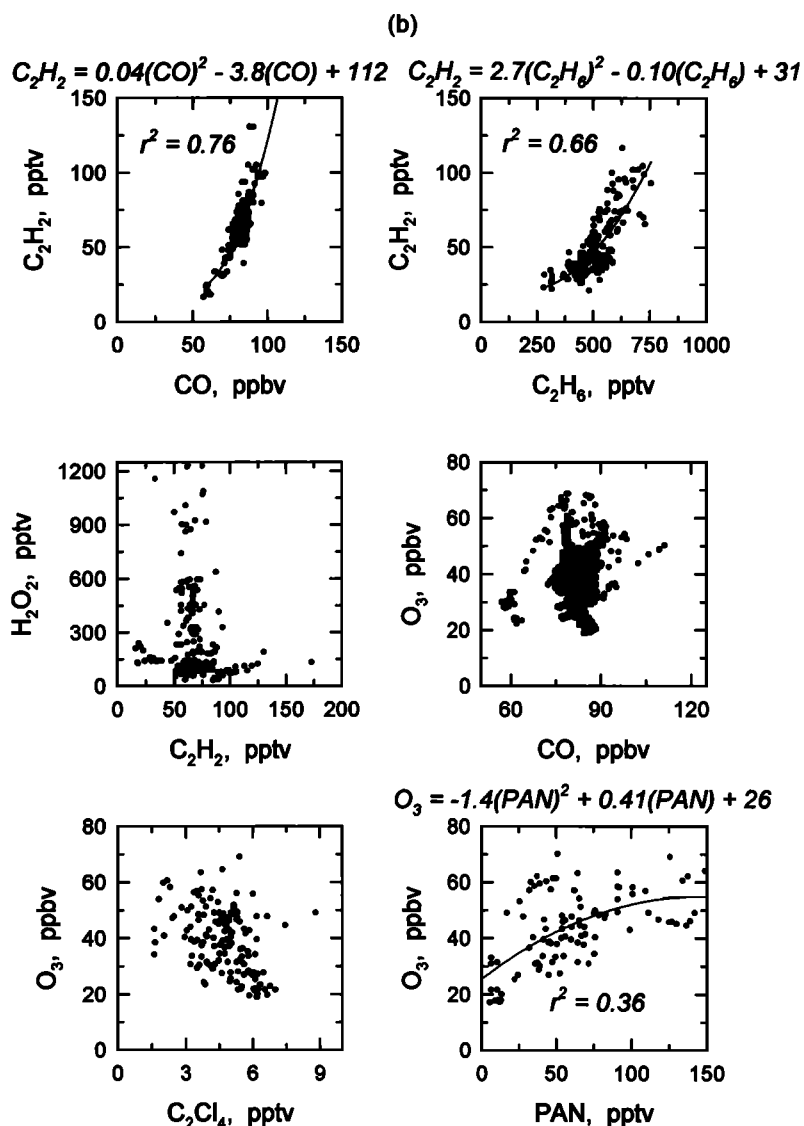


Figure 5. (continued)

between C_2H_2 and CO ($r^2 = 0.76$) and C_2H_6 ($r^2 = 0.66$). In the continental south cases the air parcels are much more aged by losses from OH oxidation and dilution by atmospheric mixing processes than the comparable continental north data [McKeen and Liu, 1993; Smyth et al., 1996]. In contrast to the continental north data, the upper tropospheric continental south air parcels do not exhibit a correlation between H_2O_2 or CH_3OOH and C_2H_2 . There was also a poor correlation between O_3 and CO. One similarity between these two upper tropospheric data sets is the modest correlation between O_3 and PAN, although it does not seem to be a simple linear one ($r^2 = 0.36$). However, in the continental south case, O_3 and C_2Cl_4 were anticorrelated. One possible explanation for these observations is the uplifting of polluted industrial emissions which then become intermixed with inputs of stratospheric air. However, the significant mixing ratios of H_2O_2 and CH_3OOH are not explained using this scenario. Perhaps these gas phase species were produced by extensive evaporation of polluted cloud waters in the upper troposphere over the equatorial Pacific. This mechanism could also be associated with the modest mixing ratios of HNO_3 and CH_3COOH in this altitude range (Figure 4b). Such a chemical signature is

consistent with a biomass burning influence [Talbot et al., 1996b]. Wood burning is known to be widespread and extensively used in the Philippines for cooking [Bensel and Remedio, 1992]. Although the upper tropospheric data did not show enhancements in CH_3Cl , the poor solubility of CH_3Cl and potential decoupling of cloud-processed air parcels could be responsible for masking more direct evidence for a biomass burning influence.

4.4. Aged Pacific Air Masses

Isentropic trajectories that had not passed over continental areas of Asia or Indonesia for the previous 5 day period occurred infrequently during PEM-West B. This is direct contrast to the fall time period, where aged marine air masses are commonly directed toward Asia by circulation around the persistent and large high pressure system in the western Pacific [Gregory et al., 1996]. During the wintertime we only encountered aged marine air during flights over the equatorial western Pacific (i.e., $<20^\circ N$ latitude). These data are summarized in Table 3 while Figures 6a, 6b, and 6c illustrate our observations for selected species. Although the data are sparse even for species measured with fast

Table 3. Mixing Ratios of Principal Species Measured in Aged (> 5 days) Marine Air Over the Western Pacific Basin

| Species | < 2 km | | | | | | 2 - 7 km | | | | | | 7 - 12 km | | | | | |
|--|--------|------|--------|-------------|-----|--|----------|------|--------|-------------|----|--|-----------|------|--------|-------------|-----|--|
| | Mean | s.d. | Median | Range | N | | Mean | s.d. | Median | Range | N | | Mean | s.d. | Median | Range | N | |
| | | | | | | | | | | | | | | | | | | |
| NO | 6.1 | 7.8 | 7.1 | 5.2-194 | 70 | | 8.0 | 3.4 | 9.3 | 2.4-11 | 19 | | 28 | 73 | 9.0 | 2.9-586 | 485 | |
| HNO ₃ | 126 | 35 | 129 | 59-176 | 18 | | 205 | 52 | 217 | 116-251 | 5 | | 115 | 82 | 88 | 34-333 | 32 | |
| PAN | 1.9 | 1.5 | 1.0 | 1.0-5.2 | 23 | | 4.2 | 0.70 | 3.4 | 3.1-5.0 | 6 | | 14 | 15 | 8.8 | 3.2-58 | 48 | |
| ΣNO _x | 141 | 69 | 141 | 66-250 | 18 | | 220 | 59 | 245 | 116-256 | 5 | | 164 | 297 | 80 | 62-2018 | 32 | |
| O ₃ | 18 | 6 | 19 | 8-27 | 253 | | 55 | 2 | 55 | 49-58 | 71 | | 23 | 8 | 20 | 16-52 | 979 | |
| CO | 92 | 16 | 98 | 52-101 | 178 | | 87 | 2 | 88 | 84-90 | 61 | | 83 | 8 | 85 | 60-93 | 873 | |
| CH ₄ | 1722 | 23 | 1725 | 1651-1746 | 164 | | 1718 | 2 | 1717 | 1714-1723 | 61 | | 1719 | 10 | 1719 | 1682-1741 | 692 | |
| CO ₂ | 358.5 | 0.80 | 358.6 | 356.1-359.2 | 119 | | 358.2 | 0.07 | 358.2 | 358.0-358.3 | 61 | | 358.3 | 0.30 | 358.4 | 357.3-358.9 | 874 | |
| N ₂ O | NA | NA | NA | NA | NA | | NA | NA | NA | NA | NA | | 312.0 | 0.40 | 311.8 | 311.1-312.8 | 97 | |
| SO ₂ | 67 | 53 | 35 | 15-163 | 26 | | 11 | 1.8 | 10 | 8-13 | 8 | | 27 | 44 | 11 | 4-241 | 95 | |
| CH ₃ SCH ₃ | 33 | 16 | 22 | 11-73 | 26 | | ND | ND | ND | ND | 8 | | 4.8 | 3.2 | 4 | 1.5-17 | 92 | |
| HCOOH | 53 | 31 | 50 | 10-133 | 22 | | 31 | 23 | 37 | 10-73 | 7 | | 99 | 83 | 68 | 10-344 | 45 | |
| CH ₃ COOH | 86 | 62 | 63 | 15-242 | 23 | | 36 | 25 | 32 | 15-82 | 7 | | 120 | 109 | 73 | 15-461 | 46 | |
| H ₂ O ₂ | 644 | 484 | 732 | 51-1393 | 36 | | 686 | 116 | 728 | 448-783 | 10 | | 369 | 176 | 367 | 100-955 | 108 | |
| CH ₃ OOH | 1049 | 286 | 1174 | 483-1427 | 36 | | 444 | 39 | 445 | 383-524 | 10 | | 444 | 191 | 501 | 49-1109 | 108 | |
| Ethane | 525 | 212 | 657 | 154-686 | 42 | | 543 | 23 | 539 | 513-598 | 11 | | 551 | 82 | 572 | 318-694 | 136 | |
| Ethene | 9.4 | 3.5 | 6.3 | 3.2-18 | 25 | | 4.7 | 0.70 | 4.1 | 3.9-5.9 | 8 | | 5.6 | 1.7 | 5.0 | 3.0-11 | 119 | |
| Propane | 44 | 17 | 51 | 12-67 | 42 | | 36 | 5.8 | 34 | 27-46 | 11 | | 46 | 16 | 43 | 14-143 | 136 | |
| i-Butane | 5.0 | 1.7 | 4.3 | 3.0-8.3 | 16 | | ND | ND | ND | ND | 11 | | 9.2 | 17 | 9.7 | 3.4-92 | 25 | |
| n-Butane | 5.1 | 2.1 | 3.5 | 3.2-12 | 24 | | 3.3 | 0.30 | 3.3 | 3.0-3.6 | 3 | | 6.9 | 5.2 | 8.5 | 3.0-40 | 59 | |
| Ethyne | 72 | 38 | 91 | 4.9-120 | 42 | | 5.6 | 4.2 | 57 | 49-61 | 11 | | 64 | 30 | 66 | 13-317 | 136 | |
| i-Pentane | ND | ND | ND | ND | 42 | | ND | ND | ND | ND | 11 | | ND | ND | ND | ND | 135 | |
| n-Pentane | ND | ND | ND | ND | 42 | | ND | ND | ND | ND | 11 | | ND | ND | ND | ND | 135 | |
| n-Hexane | ND | ND | ND | ND | 41 | | ND | ND | ND | ND | 11 | | ND | ND | ND | ND | 135 | |
| Benzene | 14 | 5.2 | 15 | 4.7-26 | 41 | | 9.4 | 3.2 | 9.6 | 5.2-14 | 11 | | 12 | 4.6 | 11 | 4.3-28 | 135 | |
| ¹¹ F | 275 | 2.2 | 275 | 270-278 | 42 | | 276 | 2.9 | 276 | 270-279 | 11 | | 273 | 1.8 | 273 | 267-278 | 136 | |
| ¹⁹ F | 518 | 3.6 | 517 | 513-525 | 42 | | 522 | 3.7 | 522 | 516-527 | 11 | | 518 | 2.5 | 518 | 506-524 | 136 | |
| ¹⁹ F | 85 | 0.87 | 84 | 82-86 | 42 | | 84 | 0.58 | 84 | 84-85 | 10 | | 84 | 1.2 | 84 | 82-88 | 132 | |
| CH ₃ CCl ₃ | 126 | 4.2 | 126 | 117-132 | 42 | | 123 | 1.9 | 123 | 120-126 | 9 | | 125 | 2.8 | 124 | 117-132 | 118 | |
| CCl ₄ | 108 | 1.0 | 108 | 107-110 | 41 | | 108 | 1.1 | 108 | 106-108 | 9 | | 108 | 1.9 | 108 | 103-112 | 119 | |
| C ₂ Cl ₄ | 5.3 | 1.7 | 6.0 | 2.1-7.7 | 42 | | 4.5 | 0.43 | 4.4 | 4.0-5.0 | 9 | | 5.0 | 0.88 | 5.0 | 3.4-7.1 | 123 | |
| C ₃ H ₈ /C ₂ H ₆ | 0.09 | 0.01 | 0.09 | 0.07-0.12 | 42 | | 0.07 | 0.01 | 0.06 | 0.05-0.09 | 11 | | 0.08 | 0.02 | 0.08 | 0.04-0.22 | 136 | |
| C ₂ H ₂ /CO | 2.1 | 2.4 | 1.1 | 0.80-9.4 | 33 | | 0.07 | 0.01 | 0.06 | 0.05-0.09 | 11 | | 1.7 | 0.83 | 1.4 | 0.28-5.1 | 128 | |
| NO ₃ ⁻ | 40 | 10 | 36 | 32-51 | 3 | | ND | ND | ND | ND | 1 | | 26 | 24 | 16 | 9.1-54 | 3 | |
| nis-SO ₄ ²⁻ | 85 | 51 | 62 | 50-144 | 3 | | 12 | NA | NA | NA | 1 | | 11 | 9.4 | 5.6 | 4.2-36 | 10 | |
| NH ₄ ⁺ | 154 | 151 | 72 | 62-328 | 3 | | ND | ND | ND | ND | 1 | | 28 | 7.4 | 23 | 21-40 | 5 | |
| ²¹⁰ Pb | 3.0 | 1.9 | 2.4 | 1.5-5.1 | 3 | | 4.2 | NA | NA | NA | 1 | | 1.2 | 0.91 | 1.1 | 0.53-2.7 | 14 | |
| ⁷ Be | 41 | 30 | 20 | 20-62 | 2 | | 105 | NA | NA | NA | 1 | | 191 | 125 | 139 | 51-506 | 11 | |
| CN | 512 | 375 | 314 | 115-4119 | 217 | | 278 | 13 | 271 | 261-337 | 49 | | 716 | 1094 | 238 | 9-12000 | 708 | |
| Aerosols | 136 | 231 | 18 | 3.7-1745 | 253 | | 108 | 140 | 0.12 | 0.01-350 | 71 | | 6.5 | 24 | 0.10 | 0.01-295 | 990 | |

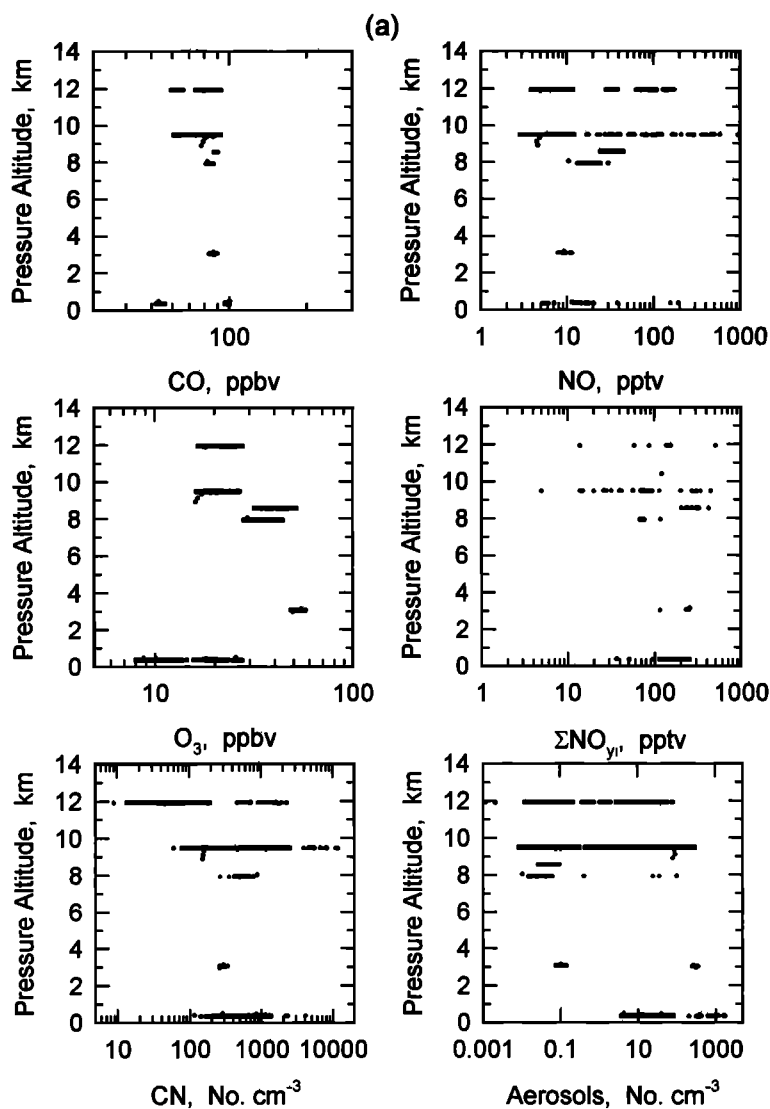


Figure 6. Vertical distributions of selected atmospheric species in aged marine air masses over the western Pacific basin. Trajectory analysis [Merrill *et al.*, this issue] indicated that these air masses had spent ≥ 5 days over the Pacific basin. Species grouping reflect (a) principal species resulting from combustion processes, (b) water-soluble species, and (c) air mass tracer species.

response sensors, a few salient features are apparent. One of the most notable is the low O_3 mixing ratios, of the order of 20 ppbv, measured at 9–12 km altitude. Remotely sensed O_3 mixing ratios showed that this situation was wide-spread and the norm in the equatorial region at this time of the year [E.V. Browell *et al.*, Ozone and aerosol distributions and air mass characteristics over the western Pacific during the late winter, submitted to *Journal of Geophysical Research*, 1996] (hereinafter referred to as Browell *et al.*, submitted manuscript, 1996). In addition, CH_3SCH_3 and CH_3I exhibited vertical distributions similar to that of O_3 , with nearly identical mixing ratios in the marine boundary layer and 9–12 km altitude [Thornton *et al.*, this issue; Blake *et al.*, this issue]. Both of these trace gases are believed to have marine biogenic sources and lifetimes against OH attack of the order of hours to days [Thornton *et al.*, this issue; Blake *et al.*, this issue]. Collectively, our observations indicate extensive and rapid vertical transport of marine boundary layer air to the upper troposphere by convective systems over the equatorial Pacific region in winter-time. This transport appears to be very important for influencing the distribution of certain species over the equatorial Pacific.

Another important influence of these convective systems may be the generation of CN aerosols and lightning-produced NO in the upper troposphere (Figure 6a) [Crawford *et al.*, this issue]. These features appear to be a common characteristic of air masses over the western Pacific that cross equatorial areas. In some cases we also observed significant mixing ratios of HNO_3 in the upper troposphere, possibly related to the NO_x source in electrically active convective clouds (Figure 6b). In the cold upper troposphere, HNO_3 should be removed primarily by photolysis with a lifetime of the order of a few weeks [Johnston *et al.*, 1974; Logan, 1983].

Like both continental source region data sets, the aged marine air cases exhibited an apparent photochemical influence near 9 km altitude. In this regard the mixing ratios of water-soluble species (Figure 6b) appear to have been replenished compared to their abundance in the continental south data set. In fact, considerably more reactive nitrogen resides as HNO_3 compared with PAN (Figure 6c), which is the opposite of what has been observed at higher northern latitudes [Singh *et al.*, 1992]. The exceptionally small mixing ratios of PAN above 9 km altitude

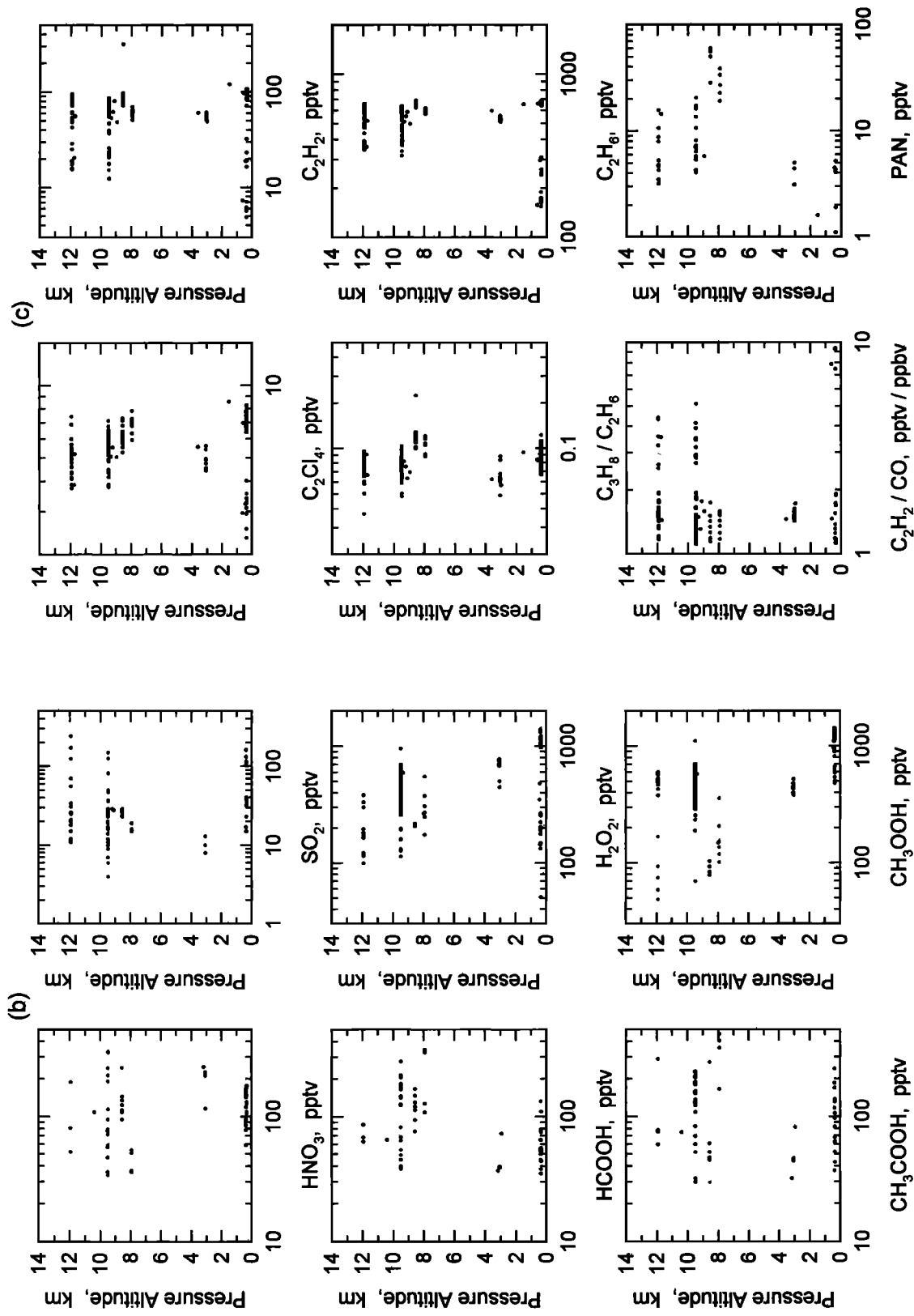


Figure 6. (continued)

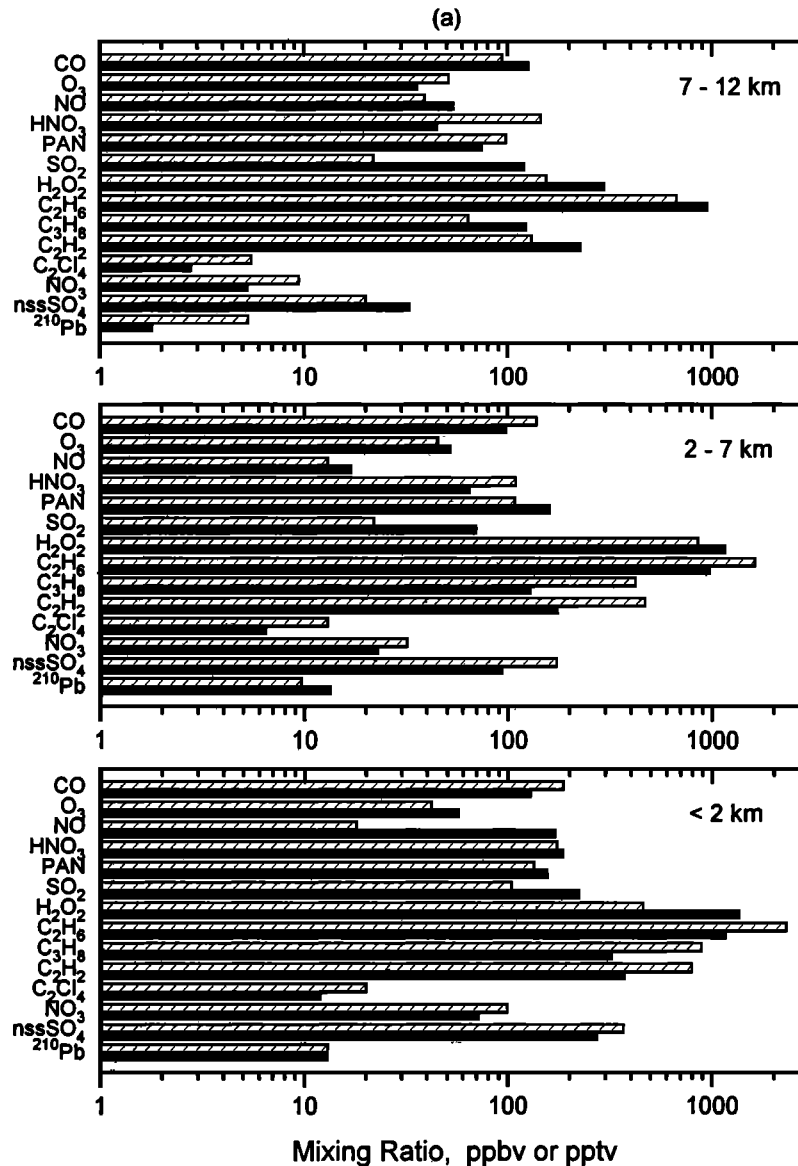


Figure 7. Comparison of median mixing ratios for selected species observed during the PEM-West A and B expeditions for air masses in the (a) continental north, (b) continental south, and (c) aged marine classifications. In Figures 7a and 7b the grey bar represents PEM-West A and the hatched PEM-West B. For Figure 7c, the grey bar represents the PEM-West A marine south data, the white bar the PEM-West A marine north data, and the PEM-West B marine (<20°N latitude) data the hatched bar. Mixing ratios of CO and O₃ are stated in parts per billion by volume, ²¹⁰Pb in fCi scm⁻¹, and the other species in parts per trillion by volume. The data used in these comparisons were obtained from this paper, Talbot *et al.* [1996], and Gregory *et al.* [1996].

most likely reflect the transport of marine boundary layer air parcels to these altitudes. Because of PAN's rapid thermal decomposition in warm air parcels, it is typically found at mixing ratios of <10 pptv in the marine boundary layer in equatorial regions [Ridley *et al.*, 1990; Singh *et al.*, 1990]. Furthermore, there is a limited reservoir of PAN precursors, such as acetone, in these air parcels [Singh *et al.*, 1995].

5. Seasonal Comparison of PEM-West A and PEM-West B Data Sets

Comparison of the PEM-West A and PEM-West B data sets is of great interest to document seasonal differences in the distribu-

tion of important tropospheric species over the vast western Pacific basin. We chose to do this by comparing median values for selected species as a function of altitude. We developed these comparisons for the continental north and south and aged marine air mass classifications. In drawing conclusions from these comparisons, one must be cautious due to the "snapshot" pictures of the atmosphere these data represent. Overall, we believe that the comparison of the two data sets is quite robust, since they were both collected from the NASA DC-8 airborne platform by an identical group of investigators using the same instruments and calibration standards. The DC-8 also flew in similar environmental conditions (e.g., mostly avoiding clouds and actively precipitating systems) over the same geographic region during both expeditions.

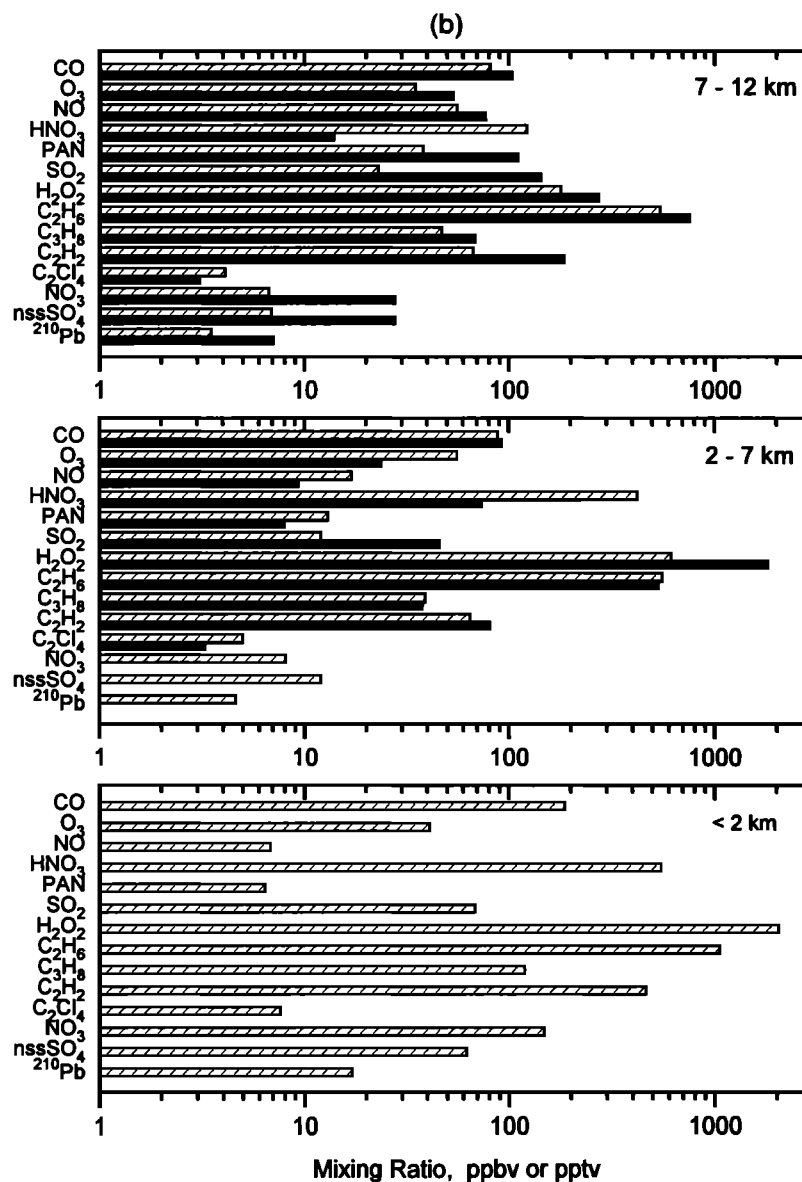


Figure 7. (continued)

5.1. Continental North Source Region

The most pronounced difference between the PEM-West A and PEM-West B data is centered on SO_2 . Sulfur dioxide mixing ratios ranged from twofold larger in the boundary layer to fourfold in the upper troposphere during PEM-West A compared with PEM-West B (Figure 7a). This result has been attributed to the eruption of Mount Pinatubo in the Philippines a few months prior to the PEM-West A expedition [Thornton *et al.*, 1996; Thornton *et al.*, this issue]. During PEM-West B, SO_2 mixing ratios were consistent with earlier measurements in the low parts per trillion by volume range [Maroulis *et al.*, 1980; Thornton and Bandy, 1993], particularly in the upper troposphere and in aged marine air parcels. The only other species that showed consistently larger mixing ratios during PEM-West A compared with PEM-West B was H_2O_2 . The largest difference occurred in the boundary layer (2.5-fold) and upper troposphere (twofold). The seasonal difference in this case was probably directly related to

enhanced photochemical activity during the late summer to early fall period (PEM-West A) compared with the wintertime (PEM-West B) [Crawford *et al.*, this issue]. Indeed, the relative abundances of H_2O_2 and CH_3OOH are believed to be a useful diagnostic for photochemical activity [Jacob *et al.*, 1995].

Mixing ratios of the hydrocarbon species C_2H_2 , C_2H_6 , C_3H_8 were on the average a factor of 2 larger during PEM-West B compared with PEM-West A. This was true for all three altitude bins. In addition, in the upper troposphere NO , HNO_3 , C_2Cl_4 , and aerosol NO_3^- and ^{210}Pb showed the same twofold enhancements. These observations may reflect a somewhat greater continental and anthropogenic impact on the upper troposphere during PEM-West A. However, other processes are probably also important for these results. Decreased photochemical activity would support smaller OH concentrations, resulting in slowed loss rates of hydrocarbons, especially for short-lived ones like C_2H_2 and C_3H_8 [Blake *et al.*, this issue]. Because CO and C_2H_6 are lost by OH oxidation at similar rates [McKeen and Liu, 1993] and the fact

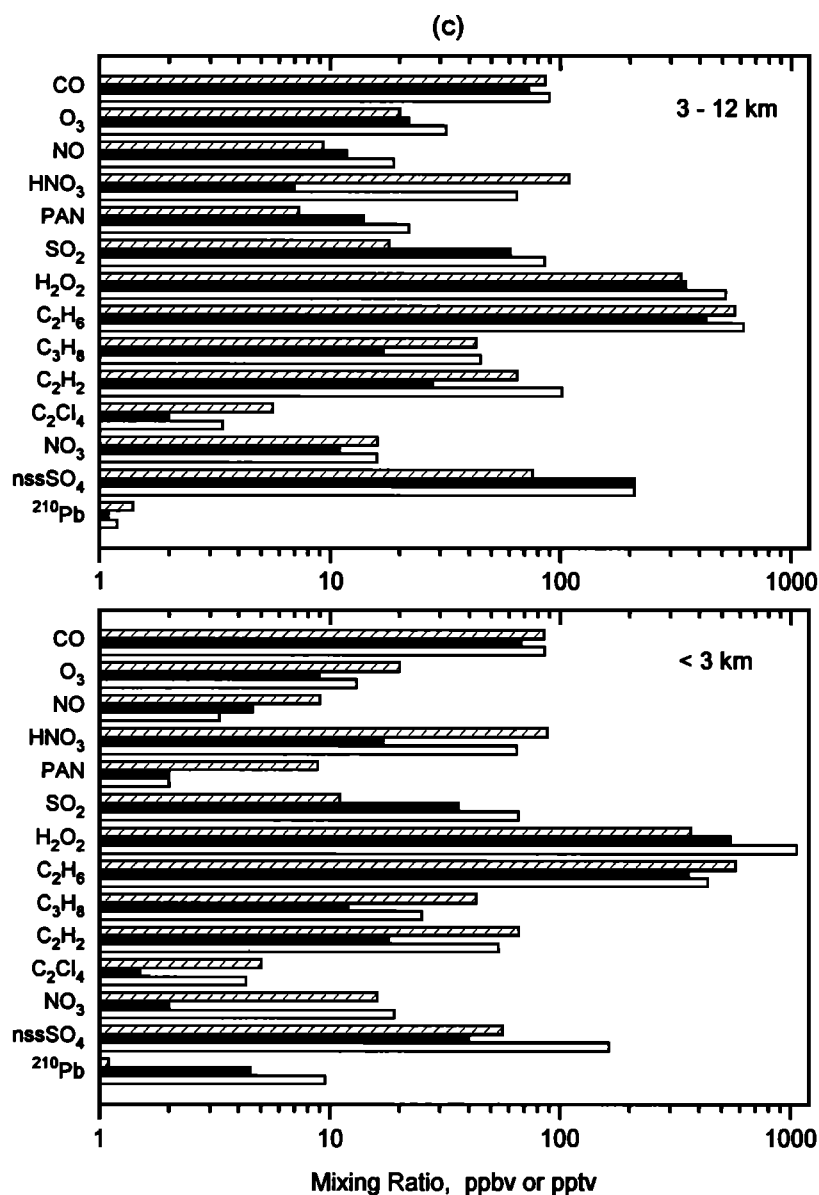


Figure 7. (continued)

that CO did not show the seasonal difference that C_2H_6 did, this suggests that photochemistry may not be the controlling factor, at least in the case of C_2H_6 .

The significantly smaller H_2O_2 mixing ratios in the upper troposphere during PEM-West B compared to PEM-West A indicates a much lowered photochemical activity, and this could contribute directly to the larger mixing ratios of NO, especially in the upper troposphere. The hydrocarbon data are consistent with this regime. For HNO_3 we propose that during PEM-West A it might have been effectively sequestered into fine particulate matter possibly through formation of nitrosyl sulfuric acid ($NOHSO_4$) related to potentially unusually large mixing ratios of H_2SO_4 associated with the Mount Pinatubo eruption [Burley and Johnston, 1992]. Significant enhancements in the H_2SO_4 mixing ratio would provide a favorable environment for extensive aerosol nucleation [Brock et al., 1995]. The details of this removal mechanism are discussed in a companion paper [Sandholm et al., 1996b]. The PEM-West B study period, as evidenced by the distribution of SO_2 , was a return to more normal chemical

environment over the western Pacific basin. Thus HNO_3 was present in larger but more typical mixing ratios [Huebert and Lazrus, 1980].

5.2. Continental South Source Region

Since we did not sample boundary layer outflow from the continental south source region during PEM-West A, the comparisons here are focused on the middle to upper troposphere. In general, the results of these seasonal comparisons were similar to those outlined for the continental north region. Sulfur dioxide mixing ratios were a factor of 2.5 greater at 2 - 7 km altitude and 6 times greater at 7 - 12 km during PEM-West A compared with PEM-West B. Again this is most likely directly related to emissions from Mount Pinatubo, which is located within the continental south source region. Similarly, H_2O_2 mixing ratios were threefold and 1.5-fold greater during PEM-West A at 2 - 7 and 7 - 12 km altitude, respectively. This would appear to be evidence that photochemical activity is reduced in wintertime in

the northern tropics and subtropics by rates analogous to those at higher northern latitudes. Notice, however, that except for C_2H_2 and C_2H_6 at 7–12 km altitude the hydrocarbon mixing ratios were remarkably comparable between the two seasons. This may indicate that source emissions might be driving the greatly enhanced hydrocarbon mixing ratios in the continental north region during PEM-West B.

In contrast to the upper tropospheric continental north data, the 7–12 km altitude range in the continental south region showed ^{210}Pb at concentrations twofold greater and aerosol NO_3^- and non-sea-salt (nss) SO_4^{2-} mixing ratios fourfold greater during PEM-West A compared from PEM-West B. This latter observation and the significantly larger mixing ratios of HNO_3 during PEM-West B compared with PEM-West A are consistent with an aerosol loss mechanism for HNO_3 during PEM-West A. Alternatively, the coincident enhancement in ^{210}Pb with NO_3^- and $nssSO_4^{2-}$ might simply reflect stronger continental inputs. This would also be consistent with the larger NO , C_2H_2 , and C_2H_6 mixing ratios in the upper troposphere during PEM-West A.

5.3. Aged Marine Air

To be consistent with the presentation of the aged marine air chemical composition during PEM-West A by Gregory *et al.* [1996a], we divided the PEM-West B data into <3 and 3–12 km altitude bins. During PEM-West A, aged marine air was sampled routinely, both in the continental north and in the south source regions. This provided enough data to develop chemical signatures for these two regions. In comparison, aged marine air was rarely sampled during PEM-West B and then only in the continental south region. The results of these three aged marine air comparisons are shown in Figure 7c. The comparisons are not unlike those for the two continental outflow source regions. The comparisons are the most dramatic for SO_2 , with PEM-West A north mixing ratios greater than the other two classifications by factors of 2 (south) to 6 (PEM-West B). Emissions from Mount Pinatubo are once again the obvious explanation. In the middle to upper troposphere, NO and PAN showed relationships comparable with those for SO_2 . However, at low-altitude NO , PAN, and HNO_3 , mixing ratios were two- to threefold greater during PEM-West B compared with PEM-West A. The reasons for these relationships are unclear, especially since CO was quite comparable between these three aged air comparisons. They may be associated with shifts in reactive nitrogen partitioning related to strong effects from Mount Pinatubo emissions during PEM-West A but minimal ones during PEM-West B.

It is noteworthy that the hydrocarbons were present in all three aged air masses in approximately equal amounts. This is further evidence that slowed loss of hydrocarbons by OH oxidation was not supporting larger mixing ratios of these species during PEM-West B. Photochemical activity was suppressed, however, based on the significantly smaller mixing ratios of H_2O_2 and CH_3OOH during PEM-West B.

6. Conclusions

We have presented a summary of the atmospheric chemical composition over the western Pacific basin during the winter of 1994. Backward 5 day isentropic trajectories were used to classify the air masses into continental north or south divisions and aged marine air. Frequent rapid outflow of continental air parcels was observed, while aged marine air was rarely encountered. This is in direct contrast to what we found during PEM-West A, where

aged marine air was recurrently sampled near Asia due to its advection around a persistent high-pressure system over the western Pacific.

We observed significant outflow of Asian continental emissions to the western Pacific basin below 5 km altitude. Industrial inputs to the continental north and south outflows were evident due to enhanced mixing ratios of common solvent vapors such C_2Cl_4 , CH_3CCl_3 , and C_6H_6 . In the upper troposphere the region between 8 and 10 km altitude was commonly influenced by continental emissions in which water-soluble species and aerosols were depleted most likely during transport through wet convective systems. This feature in the vertical distribution of species was also prevalent during PEM-West A, suggesting that it may be persistent all through the year. Over the continental north source region these upper tropospheric air masses appeared to be composed of recent combustion inputs intermixed with photochemically processed aged industrial emissions. Inputs from combustion and industrial sources were also apparent over the continental south region, but they were well aged.

A seasonal comparison of the two PEM-West data sets revealed significantly enhanced SO_2 mixing ratios during PEM-West A, presumably due to emissions associated with the eruption of Mount Pinatubo a few months prior to that expedition. A similar trend was exhibited by H_2O_2 and CH_3OOH , apparently driven by suppressed photochemical activity during wintertime. Another pronounced feature was the twofold increased hydrocarbon mixing ratios in the continental north outflow region during PEM-West B. Although decreased oxidation loss by OH could have contributed to this, we proposed that increased source emissions were probably more important. Overall, the two PEM-West data sets are remarkably comparable in chemical composition and represent important benchmark documentation of atmospheric chemistry over the western Pacific basin.

Acknowledgments. We appreciate the support provided by the DC-8 flight and ground crews at the NASA Ames Research Center. The assistance of Faith Sheridan in the preparation of this manuscript is greatly acknowledged. This research was supported by the NASA Global Tropospheric Chemistry program in the office of Mission to Planet Earth.

References

- Bensel, T. G., and E. M. Remedio, The forgotten fuel: Biomass energy in the Philippine economy, *Philipp. Q. Cult. Soc.*, 20, 24–48, 1992.
- Blake, N. J., Blake, D. R., B. C. Sive, T.-Y. Chen, F. S. Rowland, J. E. Collins Jr., G. W. Sachse, and B. E. Anderson, Biomass burning and vertical distribution of atmospheric methyl halides and other reduced carbon gases in the South Atlantic region, *J. Geophys. Res.*, 101, 24,151–24,164, 1996.
- Blake, N. J., D. R. Blake, T.-Y. Chen, J. E. Collins Jr., G. W. Sachse, B. E. Anderson, and F. S. Rowland, Distribution and seasonality of selected hydrocarbons and halocarbons over the western Pacific basin during PEM-West A and PEM-West B, *J. Geophys. Res.*, this issue.
- Brock, C. A., P. Hamill, J. C. Wilson, H. H. Jonsson, and K. R. Chan, Particle formation in the upper tropical troposphere: A source of nuclei for the stratospheric aerosol, *Science*, 270, 1650–1653, 1995.
- Burley, J. D., and H. S. Johnston, Nitrosyl sulfuric acid and stratospheric aerosols, *Geophys. Res. Lett.*, 19, 1363–1366, 1992.
- Crawford, J., *et al.*, Implications of large-scale shift in tropospheric NO_2 levels in the remote tropical Pacific, *J. Geophys. Res.*, this issue.
- Dibb, J. E., R. W. Talbot, K. I. Klemm, G. L. Gregory, H. B. Singh, J. D. Bradshaw, and S. T. Sandholm, Asian influence over the western North Pacific during the fall season: Inferences from lead-210, soluble ionic species, and ozone, *J. Geophys. Res.*, 101, 1779–1792, 1996.
- Dibb, J. E., R. W. Talbot, B. L. Lefter, E. Scheuer, G. L. Gregory, E. V. Browell, J. D. Bradshaw, S. T. Sandholm, and H. B. Singh, Distribution of ^{7}Be , ^{210}Pb and soluble aerosol-associated ionic species over the western Pacific: PEM-West B, February - March 1994, *J. Geophys. Res.*, this issue.

- Duce, R. A., C. K. Unni, B. J. Ray, J. M. Prospero, and J. T. Merrill, Long-range atmospheric transport of soil dust from Asia to the tropical North Pacific: Temporal variability, *Science*, 209, 1522-1524, 1980.
- Ehhalt, D. W., F. Rohrer, and A. Wahner, Sources and distribution of NO_x in the upper troposphere at northern midlatitudes, *J. Geophys. Res.*, 97, 9781-9793, 1992.
- Gao, Y., R. Arimoto, M. Y. Zhou, J. T. Merrill, and R. A. Duce, Relationships between dust concentrations over eastern Asia and the remote North Pacific, *J. Geophys. Res.*, 97, 9867-9872, 1992.
- Gregory, G. L., A. S. Bachmeier, D. R. Blake, B. G. Heikes, D. C. Thornton, J. D. Bradshaw, and Y. Kondo, Chemical signatures of aged Pacific marine air: Mixed layer and free troposphere as measured during PEM West-A, *J. Geophys. Res.*, 101, 1727-1742, 1996a.
- Gregory, G. L., J. T. Merrill, M. C. Shipham, D. R. Blake, G. W. Sachse, and H. B. Singh, Chemical characteristics of tropospheric air over the Pacific Ocean as measured during PEM-West B: Relationship to Asian outflow and trajectory history, *J. Geophys. Res.*, this issue.
- Heikes, B. G., Formaldehyde and hydroperoxides at Mauna Loa Observatory, *J. Geophys. Res.*, 97, 18,001-18,013, 1992.
- Hoell, J. M., D. D. Davis, S. C. Liu, R. Newell, H. Akimoto, R. J. McNeal, and R. J. Bendura, The Pacific Exploratory Mission-West (Phase B): February-March 1994, *J. Geophys. Res.*, this issue, 1997.
- Huebert, B. J., and A. L. Lazrus, Tropospheric gas phase and particulate nitrate measurements, *J. Geophys. Res.*, 85, 7322-7328, 1980.
- Jacob, D. J., L. W. Horowitz, J. W. Munger, B. G. Heikes, R. R. Dickerson, R. S. Artz, and W. C. Keene, Seasonal transition from NO_x-to hydrocarbon-limited conditions for ozone production over the eastern United States, *J. Geophys. Res.*, 100, 9315-9324, 1995.
- Johnston, H. S., S. -G. Chang, and G. Whitten, Photolysis of nitric acid vapor, *J. Phys. Chem.*, 78, 1-7, 1974.
- Kondo, Y., et al., Profiles and partitioning of reactive nitrogen over the Pacific Ocean in winter and early spring, *J. Geophys. Res.*, this issue.
- Kritz, M. A., J. -C. Le Roulley, and E. F. Danielsen, The China Clipper - Fast advective transport of radon-rich air from the Asian boundary layer to the upper troposphere near California, *Tellus, Ser. B*, 42, 46-61, 1990.
- Logan, J. A., Nitrogen oxides in the troposphere: Global and regional budgets, *J. Geophys. Res.*, 88, 10,785-10,807, 1983.
- Maroulis, P. J., A. L. Torres, A. B. Goldberg, and A. R. Bandy, Atmospheric SO₂ measurements on project GAMETAG, *J. Geophys. Res.*, 85, 7345-7349, 1980.
- McKeen, S. A., and S. C. Liu, Hydrocarbon ratios and photochemical history of air masses, *Geophys. Res. Lett.*, 20, 2363-2366, 1993.
- Merrill, J. T., Atmospheric long range transport to the Pacific Ocean, in *Chemical Oceanography*, edited by J. P. Riley and R. Duce, pp. 15-50, Academic, San Diego, Calif., 1989.
- Merrill, J. T., R.E. Newell, and A.S. Bachmeier, A meteorological overview for the Pacific Exploratory Mission-West, Phase B, *J. Geophys. Res.*, this issue.
- Merrill, J. T., M. Uematsu, and R. Bleck, Meteorological analysis of long range transport of mineral aerosols over the North Pacific, *J. Geophys. Res.*, 94, 8584-8598, 1989.
- Prospero, J. M., D. Savoie, R. T. Nees, R. A. Duce, and J. T. Merrill, Particulate sulfate and nitrate in the boundary layer over the North Pacific Ocean, *J. Geophys. Res.*, 90, 10,586-10,596, 1985.
- Ridley, B. A., et al., Ratios of peroxyacetyl nitrate to active nitrogen observed during aircraft flights over the eastern Pacific Ocean and continental United States, *J. Geophys. Res.*, 95, 10,179-10,192, 1990.
- Sandholm, S. T., et al., Air mass classification schemes: A comparative study of PEM-West A and PEM-West B, *J. Geophys. Res.*, 1996.
- Sandholm, S.T., J.D. Bradshaw, R.W. Talbot, H.B. Singh, G.L. Gregory, G.W. Sachse, and D.R. Blake, Comparison of N₂O₅ budgets from NASA's ABL3, PEM-West, and TRACE A measurement programs: An update, *J. Geophys. Res.*, 1996b.
- Singh, H. B., et al., Peroxyacetyl nitrate measurements during CITE 2: Atmospheric distribution and precursor relationships, *J. Geophys. Res.*, 95, 10,163-10,178, 1990.
- Singh, H. B., D. O'Hara, D. Herlth, J. D. Bradshaw, S. T. Sandholm, G. L. Gregory, G. W. Sachse, D. R. Blake, P. J. Crutzen, and M. Kanakidou, Atmospheric measurements of peroxyacetyl nitrate and other organic nitrates at high latitudes: Possible sources and sinks, *J. Geophys. Res.*, 97, 16,511-16,522, 1992.
- Singh, H. B., M. Kanakidou, and P. J. Crutzen, High concentrations and photochemical fate of carbonyls and alcohols in the global troposphere, *Nature*, 378, 50-54, 1995.
- Smyth, S., et al., Comparison of free tropospheric western Pacific air mass classification schemes for the PEM-West A experiment, *J. Geophys. Res.*, 101, 1743-1762, 1996.
- Talbot, R. W., et al., Chemical characteristics of continental outflow from Asia to the troposphere over the western Pacific Ocean during February-March 1994: Results from PEM-West A, *J. Geophys. Res.*, 101, 1713-1725, 1996a.
- Talbot, R. W., et al., Chemical characteristics of continental outflow over the tropical South Atlantic Ocean from Brazil and Africa, *J. Geophys. Res.*, 101, 24,187-24, 202, 1996b.
- Thornton, D. C., and A. R. Bandy, Sulfur dioxide and dimethyl sulfide in the central Pacific troposphere, *J. Atmos. Chem.*, 17, 1-13, 1993.
- Thornton, D. C., A. R. Bandy, B. W. Blomquist, D. D. Davis, and R. W. Talbot, Sulfur dioxide as a source of CN in the upper troposphere of the Pacific Ocean, *J. Geophys. Res.*, 101, 1883-1890, 1996.
- Thornton, D. C., A. Bandy, B. W. Blomquist, J. D. Bradshaw, and D. R. Blake, Vertical transport of sulfur dioxide and dimethyl sulfide in deep convection and its role in new particle formation, *J. Geophys. Res.*, this issue.
- Wang, C. J. -L., D. R. Blake, and F. S. Rowland, Seasonal variations in the atmospheric distribution of a reactive chlorine compound, tetrachloroethene (CCl₂=CCl₂), *Geophys. Res. Lett.*, 22, 1097-1100, 1995.

B.E. Anderson, J.E. Collins Jr., G.L. Gregory, and G.W. Sachse, NASA Langley Research Center, Hampton, VA, 23665.

A. R. Bandy and D.C. Thornton, Department of Chemistry, Drexel University, Philadelphia, PA, 19104.

D.R. Blake and N.J. Blake, Department of Chemistry, University of California, Irvine, CA, 92716.

J.D. Bradshaw and S.T. Sandholm, School of Earth and Atmospheric Sciences, Georgia Institute of Technology, Atlanta, GA, 30332.

J.E. Dibb, B.L. Lefer, and R.W. Talbot, Institute for the Study of Earth, Oceans, and Space, University of New Hampshire, Durham, NH, 03824.

G. Heikes, Center for Atmospheric Chemistry, University of Rhode Island, Narragansett, RI, 02882.

J.T. Merrill, R.F. Pueschel, and H.B. Singh, NASA Ames Research Center, Moffett Field, CA, 94035.

(Received January 13, 1996; revised June 28, 1996; accepted June 30, 1996.)